

AD-A072 050

NAVAL POSTGRADUATE SCHOOL MONTEREY CA
CONVERGENCE ZONE PREDICTION MODELS WITH PROGRAMS FOR USE ON HP---ETC(U)
MAR 79 R L BADGER

F/G 9/2

HP---ETC(U)

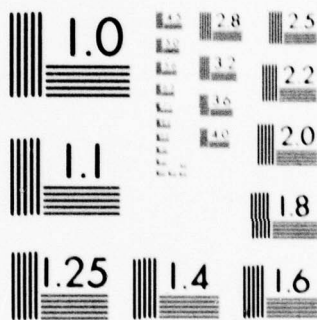
UNCLASSIFIED

NL

1 OF 2

AD
A072050





MICROCOPY RESOLUTION TEST CHART
NATIONAL BUREAU OF STANDARDS-1963-A

AD A 072050

DDC FILE COPY

LEVEL
NAVAL POSTGRADUATE SCHOOL
Monterey, California

2
B.S.



DDC
RECEIVED
JUL 30 1979
C

THESIS

CONVERGENCE ZONE PREDICTION MODELS
with Programs for Use on HP-67 and HP-97
Programmable Calculators

by

Richard L. Badger

March 1979

Thesis Advisor

A.B. Coppens

Approved for public release; distribution unlimited.

79 07 -30-133

UNCLASSIFIED

SECURITY CLASSIFICATION OF THIS PAGE (When Data Entered)

REPORT DOCUMENTATION PAGE		READ INSTRUCTIONS BEFORE COMPLETING FORM
1. REPORT NUMBER	2. GOVT ACCESSION NO.	3. RECIPIENT'S CATALOG NUMBER
4. TITLE (and Subtitle) CONVERGENCE ZONE PREDICTION MODELS With Programs for Use on HP-67 and HP-97 Programmable Calculators.		5. TYPE OF REPORT & PERIOD COVERED Master's Thesis March 1979
7. AUTHOR(s) Richard L. Badger		6. PERFORMING ORG. REPORT NUMBER
8. PERFORMING ORGANIZATION NAME AND ADDRESS Naval Postgraduate School Monterey, California 93940		9. CONTRACT OR GRANT NUMBER(s)
11. CONTROLLING OFFICE NAME AND ADDRESS Naval Postgraduate School Monterey, California 93940		10. PROGRAM ELEMENT, PROJECT, TASK AREA & WORK UNIT NUMBERS
14. MONITORING AGENCY NAME & ADDRESS (if different from Controlling Office) Naval Postgraduate School Monterey, California 93940		12. REPORT DATE March 1979
		13. NUMBER OF PAGES 99
		15. SECURITY CLASS. (of this report) Unclassified
		16a. DECLASSIFICATION/DOWNGRADING SCHEDULE
16. DISTRIBUTION STATEMENT (of this Report) Approved for public release; distribution unlimited.		
17. DISTRIBUTION STATEMENT (of the abstract entered in Block 20, if different from Report)		
18. SUPPLEMENTARY NOTES		
19. KEY WORDS (Continue on reverse side if necessary and identify by block number) Convergence Zone Transmission Loss Handheld Calculator Ray Tracing Model		
20. ABSTRACT (Continue on reverse side if necessary and identify by block number) Convergence zone (CZ) prediction models are developed based on acoustic ray tracing theory as applied to linearly segmented sound velocity profiles (SVP). The models were developed into three calculator programs, two for CZ range predictions under different source and receiver depth conditions and one for CZ gain and transmission loss (TL) predictions. The performance of the models as programmed on Hewlett-Packard HP-67 or HP-97 programmable calculators was compared to the Fast Asymptotic Coherent Transmission (FACT)		

251450 1

UNCLASSIFIED

SECURITY CLASSIFICATION OF THIS PAGE/When Data Entered:

model which is based on similar but more elaborate theory and which is designed for use on large digital computers. Agreement of the calculator programs with the FACT model is fairly good when conditions are within the design limitations of the programs and environmental conditions are not unusual.

K

Accession For	
NTIC G&AI	<input checked="checked" type="checkbox"/>
LDC TAB	<input type="checkbox"/>
Unannounced	<input type="checkbox"/>
Justification	
By _____	
Distribution/ _____	
Availability Codes	
Dist	Avail and/or special
A	

Approved for public release; distribution unlimited.

CONVERGENCE ZONE PREDICTION MODELS
with Programs for Use on HP-67 and HP-97
Programmable Calculators

by

Richard L. Badger
Lieutenant Commander, United States Navy
B.S., United States Naval Academy, 1966

Submitted in partial fulfillment of the
requirements for the degree of

MASTER OF SCIENCE IN SYSTEMS TECHNOLOGY

from the
NAVAL POSTGRADUATE SCHOOL
March 1979

Author

R. L. Badger

Approved by

Alan B. Cooper

Thesis Advisor

Ken H. Shugart

Co-Advisor

W. J. Turner

Chairman, ASW Academic Group

Jack R. Brinkley

Academic Dean

ABSTRACT

Convergence zone (CZ) prediction models are developed based on acoustic ray tracing theory as applied to linearly segmented sound velocity profiles (SVP). The models were developed into three calculator programs, two for CZ range predictions under different source and receiver depth conditions and one for CZ gain and transmission loss (TL) predictions. The performance of the models as programmed on Hewlett-Packard HP-67 or HP-97 programmable calculators was compared to the Fast Asymptotic Coherent Transmission (FACT) model which is based on similar but more elaborate theory and which is designed for use on large digital computers. Agreement of the calculator programs with the FACT model is fairly good when conditions are within the design limitations of the programs and environmental conditions are not unusual.

TABLE OF CONTENTS

I.	THE NEED FOR GOOD CZ PREDICTIONS-----	11
A.	THE PROBLEM OF THE AIRBORNE ASW UNIT-----	11
B.	ARE LARGE COMPUTERS NECESSARY?-----	12
C.	DESIRABLE CHARACTERISTICS OF A CALCULATOR PROGRAM FOR CZ PREDICTIONS-----	13
II.	USING ICAPS AS THE STANDARD FOR COMPARISON-----	15
A.	RATIONALE FOR ONLY ONE LOCATION PER OCEAN BASIN-----	15
B.	DESCRIPTION OF ICAPS-----	15
C.	DESCRIPTION OF HISTORICAL ENVIRONMENTAL DATA FILES-----	16
D.	COMPARISON OF DEEP SOUND CHANNEL CHARACTERISTICS-----	29
E.	COMPARISON OF CZ CHARACTERISTICS IN THREE OCEANS-----	31
	1. Method Used in Obtaining Data for Comparison-----	31
	2. CZ Range and Width Analysis-----	32
	3. CZ Gain and Transmission Loss Analysis-----	39
III.	CZ RAY THEORY ANALYSIS AND MODEL DEVELOPMENT-----	47
A.	CZ RANGE AND WIDTH-----	47
B.	RANGE AND WIDTH MODEL-----	50
C.	CZ GAIN AND TRANSMISSION MODEL-----	59
D.	CALCULATOR PREDICTIONS COMPARED TO ICAPS-----	66
	1. Choosing the SVP Points for the Program-----	66
	2. CZ Range and Annulus Width Comparisons-----	68
	3. CZ Gain Comparisons-----	74

IV. CONCLUSIONS-----	78
A. LIMITATIONS OF THE MODEL DEVELOPED-----	78
B. USEFULNESS OF THE MODEL DEVELOPED-----	79
APPENDIX - HP-67/97 Calculator Programs for Convergence Zone Range, Width and Transmission Loss Predictions-----	83
LIST OF REFERENCES-----	97
INITIAL DISTRIBUTION LIST-----	98

LIST OF TABLES

I.	ICAPS CZ Range & Width Data-----	33-38
II.	ICAPS CZ Gain Data Observed at the Pacific Ocean Location-----	44-45
III.	ICAPS 300Hz CZ Gain Data Observed at Atlantic & Mediterranean Locations-----	46
IV.	Five Point Sound Velocity Profiles-----	67
V.	CZ Gain Prediction Comparisons-----	75

LIST OF FIGURES

1.	ICAPS Sound Velocity Profiles-----	17-28
2.	Comparison of Pacific, Atlantic, and Mediterranean Deep Sound Channel Characteristics-----	30
3.	Estimating Transmission Loss in a CZ Annulus from an ICAPS TL Profile-----	41
4.	Sound Rays of Interest in CZ Propagation-----	48
5.	Horizontal Distance Traveled Within an Isogradient Layer-----	54
6.	RCZi and RCZo for Deep/Deep, Shal/Shal, and Crosslayer Cases-----	57-58
7.	Geometric Transmission Loss by Ray Tracing Method-----	61
8.	Determining Angular Terms for CZ Gain Algorithm-----	64
9.	Comparisons of ICAPS and Calculator CZ Annuli Predictions-----	70-72

LIST OF SYMBOLS AND DEFINITIONS

a	Attenuation coefficient (dB/m).
$C_0, C_1, C_2, \dots, C_i$	Sound velocities at various points on a linearly segmented sound velocity profile.
C_R	Sound velocity at the receiver depth.
C_S	Sound velocity at the sound source depth.
CZ	Convergence zone.
CZW	Width of the convergence zone annulus.
$D_0, D_1, D_2, \dots, D_i$	Depths of various points on a linearly segmented sound velocity profile.
D_R	Depth of the acoustic receiver.
D_S	Depth of the sound source.
DSC	Deep Sound Channel.
$\Delta r_0, \Delta r_1, \dots, \Delta r_i$	Horizontal distances traveled by a sound ray in traversing various layers of a linearly segmented sound velocity profile.
$\Delta r_S, \Delta r_R$	Horizontal range corrections made to sound ray cycle ranges to correct for source and receiver depth separation from the sonic layer depth.
$\Delta\theta$	The angular spread of all sound rays departing a sound source which result in convergence zone propagation.
f	Frequency (Hz).
G	Convergence zone gain (dB).
$g_0, g_1, g_2, \dots, g_i$	Sound velocity gradients in a linearly segmented sound velocity profile.
ML	Mixed Layer. The upper, generally isothermal, slightly positive sound velocity gradient layer of the ocean.
R	The radius of curvature of a sound ray in an isogradient layer.

R0,R1,...,R9;
S0,S1,...,S9;
RA,RB,...,RE

Data storage registers in the HP-67 or HP-97 calculators.

RCZi

Horizontal range from a sound source to the inner edge of a convergence zone annulus.

RCZo

Horizontal range from a sound source to the outer edge of a convergence zone annulus.

r

The cycle distance of a sound ray which experiences convergence zone refraction. It is a horizontal distance measured from the point of departure from the SLD to the point of return to the SLD.

r_0

The cycle distance for a ray which departs the SLD at zero degrees depression angle from the horizontal.

r_{\min}

The minimum cycle distance of all sound rays experiencing CZ refraction.

r_{rswp}

The cycle distance of a sound ray which equals r_0 but which has a positive depression angle from the horizontal at the SLD. The rays with depression angles between those for r_0 and r_{rswp} produce the reswept region in a CZ.

r_w

The working cycle distance used in a calculator program when iterating to find a particular r.

SLD

Sonic Layer Depth. The depth of maximum sound velocity above the DSC axis.

TL

Transmission Loss (dB).

TL_n

The TL in the n^{th} CZ annulus.

θ_{SLD}

The angle of departure of a sound ray from the SLD measured downward from the horizontal.

θ_{rmin}

The angle of departure of the CZ sound ray with minimum cycle distance.

θ_{rswp}	The angle of departure of the CZ sound ray which completes the CZ reswept region.
θ_{RO}	The angle of arrival of a sound ray at the receiver which departed the SLD at zero depression angle.
θ_{RR}	The angle of arrival of a sound ray at the receiver which departed the SLD at θ_{rswp} .
θ_{SO}	The angle of departure of a sound ray from the sound source which reaches the SLD at zero depression angle.
θ_{SR}	The angle of departure of a sound ray from the sound source which crosses the SLD at θ_{rswp} .
θ_{w}	θ_{SLD} in an iterative calculator routine when searching for r_{min} or θ_{rswp} .
θ_1	The average angle of departure of the sound rays within $\Delta\theta$.
θ_2	The average angle of arrival of CZ sound rays at the receiver depth.

I. THE NEED FOR GOOD CZ PREDICTIONS

A. THE PROBLEM OF THE AIRBORNE ASW UNIT

In most of the Pacific Ocean and much of the Atlantic Ocean and Mediterranean Sea, convergence zone (CZ) conditions exist a majority of the time, and they provide passive acoustic sensors with an important means of detecting sounds emitted from submarine targets. In some areas the CZ regions are the most important contact regions considered in planning acoustic searches. Obtaining accurate predictions of CZ sound propagation is therefore vital to the success of acoustic sensor tactical planners.

Currently, the primary source of acoustic predictions for U. S. Navy units is the Fleet Numerical Weather Center, Monterey, California. Propagation loss profiles for four standard frequencies and three source and receiver depth combinations are normally provided in the ASW Range Prediction System (ASRAPs) to air ASW units when requested. The profiles, showing transmission loss (TL) versus distance, are generated on a large digital computer which uses the Fast Asymptotic Coherent Transmission (FACT) model. This model uses as inputs a linearly segmented sound velocity profile (SVP), source and receiver depths, and frequencies of interest. The SVP used can be specified by the user or can come from information stored at FNWC in the form of historical data. This stored data is updated by bathythermograph (BT) reports through a complex weighting scheme as the

reports are received. Without going into further detail, it can be stated that predictions produced are only as good as the data and the computer model used, and only as timely as communications allow.

When entering a search area, a problem often arises concerning the TL profiles obtained from FNWC. Upon taking a BT measurement, the unit often finds the BT profile used to generate the acoustic predictions does not agree with the actual BT conditions in the area. If this situation occurs, the unit tends to lose confidence in the accuracy of the predictions and tactical effectiveness is felt to be diminished by lack of good information. The objective of this study was, therefore, to investigate what could be done with state-of-the-art programmable calculators to improve on the in situ convergence zone predictions available to air ASW units.

The reader only interested in the calculator programs developed may skip immediately to the appendix.

B. ARE LARGE COMPUTERS NECESSARY?

In section 5.6 of Ref. 1, Principles of Underwater Sound, by R.J. Urick, the author discusses the relative merits of two theoretical approaches to obtaining wave equation solutions in order to describe the distribution of sound energy in space and time. Several references are made to the need for digital computers to produce sound propagation descriptions with either theory. Since those comments were made,

however, there has been a revolution in the capabilities of small programmable calculators. Although it is probably true that computers are required to produce a complete description of sound propagation in the ocean with one program, calculators are capable of solving the different modes of propagation one at a time with separate programs to obtain a composite description. Examples of simple but fairly adequate calculator programs for surface duct, bottom bounce, reliable acoustic path, and deep sound channel propagation modes are contained in Refs. 2 and 3. These references also contain simple models for CZ propagation, but they are based on a mix of ray theory, rule-of-thumb, and empirical data. It was felt that a better CZ model needed to be developed.

C. DESIRABLE CHARACTERISTICS OF A CALCULATOR PROGRAM FOR CZ PREDICTIONS

1. The program should require a minimum of easily available input data. The only information not currently available but which would be needed by an airborne ASW unit is an SVP from the permanent thermocline to the ocean bottom in the unit's search area. A chart of this data could easily be included in the environmental package carried aboard the aircraft.

2. The program should be easy to operate and not require the operator to have a great deal of insight into the mathematical model or the internal operations of the calculator.

3. The output should provide ranges to the inner and outer edges of all CZ annuli of interest. It should also present the expected TL for all frequencies of interest in each annulus.

4. The run time of the program should be relatively short. This characteristic recognizes that time is important to an on-station unit.

5. The program should be based on generally accepted acoustic theory. This characteristic is desirable because a user would probably have more confidence in such a model than one based on empirical data and thus applicable only to a specific ocean basin. With empirical models, the user often wonders if the area he intends to search corresponds to the mean set of conditions used to generate the model or is somehow different.

6. Ideally, the program's performance should agree closely with the generally accepted large computer models currently in use.

II. USING ICAPS AS THE STANDARD FOR COMPARISON

A. RATIONALE FOR ONLY ONE LOCATION PER OCEAN BASIN

As will be demonstrated, the CZ characteristics of the three locations studied vary considerably. The deep sound channels which produce CZ phenomena are quite different as are the ranges from source to CZ annuli. The objective of this study was to produce a mathematical model for CZ predictions for use on small programmable calculators. It was reasoned that if the model would work for the different conditions of the three locations studied, it would work for all of the variations to be expected within any one of the ocean areas.

B. DESCRIPTION OF ICAPS

The Integrated Carrier ASW Prediction System (ICAPS) is a passive and active acoustic prediction system developed for installation aboard aircraft carriers and other large naval vessels which have digital computers. It contains four sets of historical environmental data, one each for the North Pacific, North Atlantic, and Indian Oceans, and one for the Mediterranean and Black Seas. It also contains several production programs for predicting naval sonar system performance. The FACT model is used in the passive sensor predictions. This is the same model used at FNWC for ASRAPs. Reference 4 contains a description of the installation and operation of ICAPS in the IBM 360 Computer Center at the

Naval Postgraduate School. Reference 5 contains a description of the mathematics used in the FACT model.

C. DESCRIPTION OF HISTORICAL ENVIRONMENTAL DATA FILES

Figures 1(a) through 1(l) depict twelve sound velocity profiles produced by ICAPS from its historical environmental data files. Figures 1(a) through 1(d) show SVP information for the months of February, May, August, and November for 40N 140W in the Pacific Ocean. Figures 1(e) through 1(h) are the same information for 31N 69W in the Atlantic Ocean, and likewise, Figures 1(i) through 1(l) are for 36N 18E in the Mediterranean Sea.

The historical data files used to produce these profiles consist of temperature and salinity values for over thirty depths, for four seasons of the year, and for many locations spaced at one to five degree latitude and longitude intervals in each ocean area covered. When specific latitude, longitude, and date are specified, interpolations are performed to produce the approximate temperature and salinity profiles to be expected at that location and date. This information is then converted to an SVP. The output from this portion of the system consists of seven columns of values, one each for depth in meters and feet, temperature in Celsius and Fahrenheit, salinity, and sound velocity in meters per second and feet per second. The depths associated with these quantities begin at ten meter intervals near the ocean surface and gradually increase through 25, 50, 100, 250, 500, and 1,000 meter intervals as depth increases. The last line

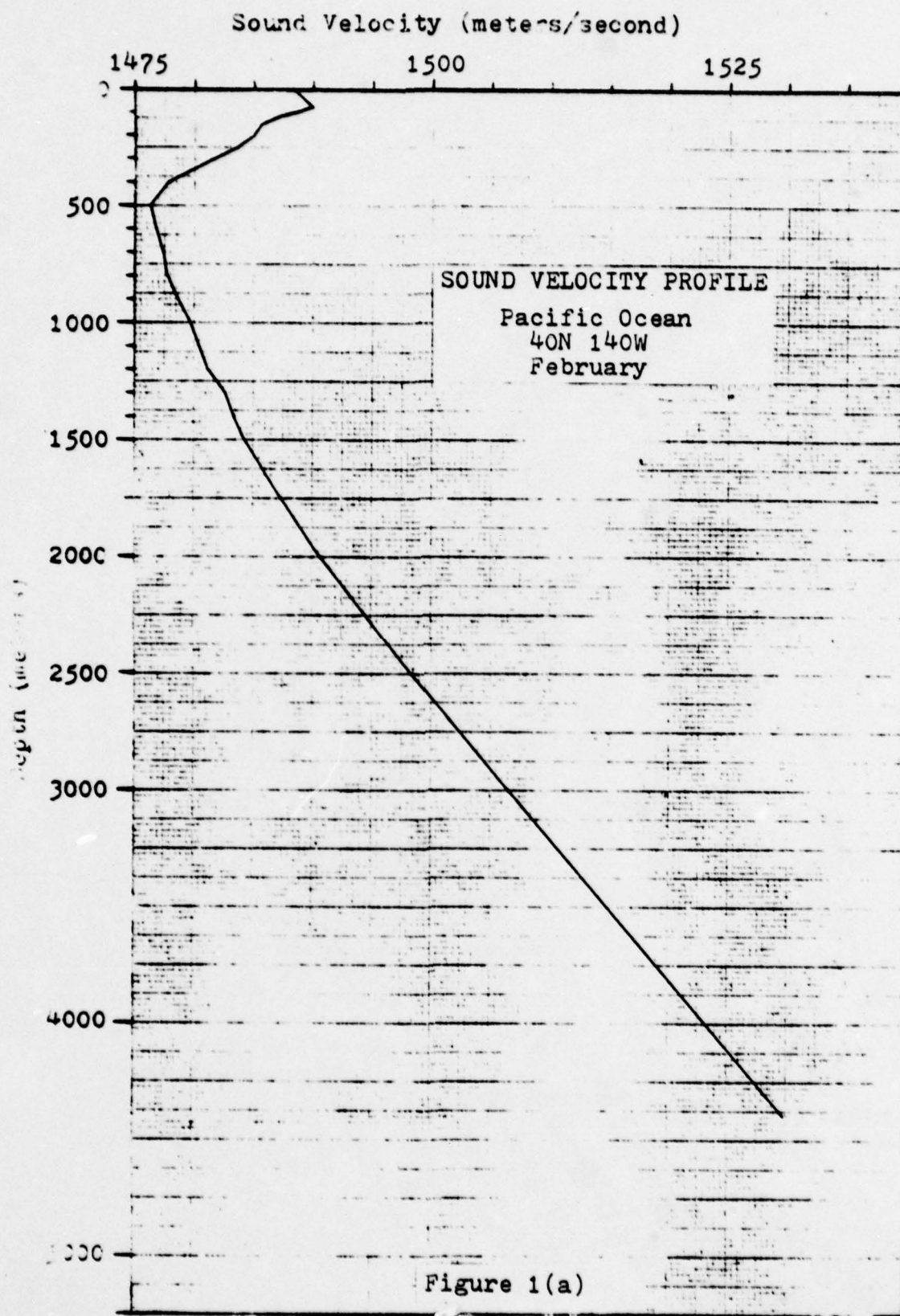
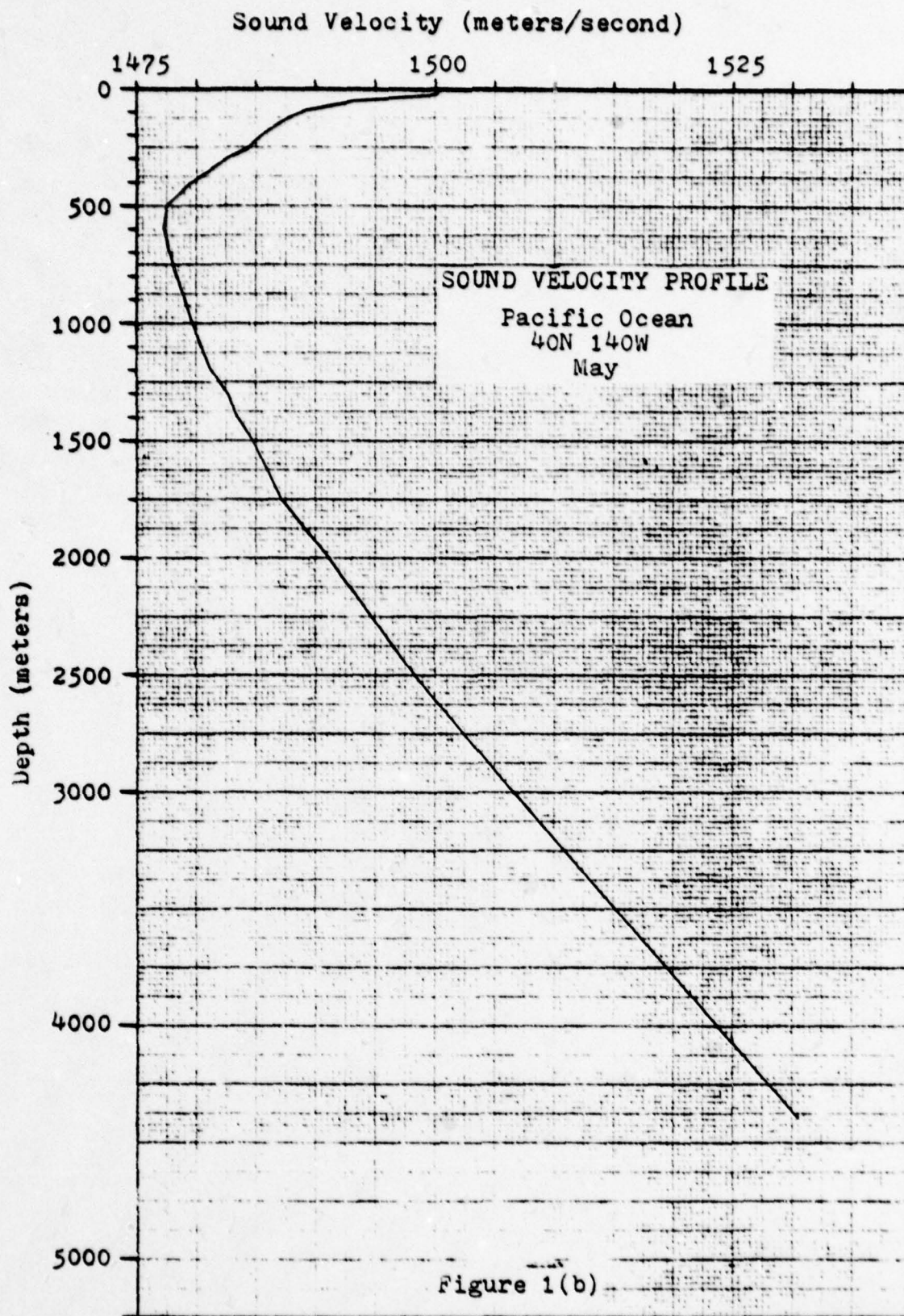
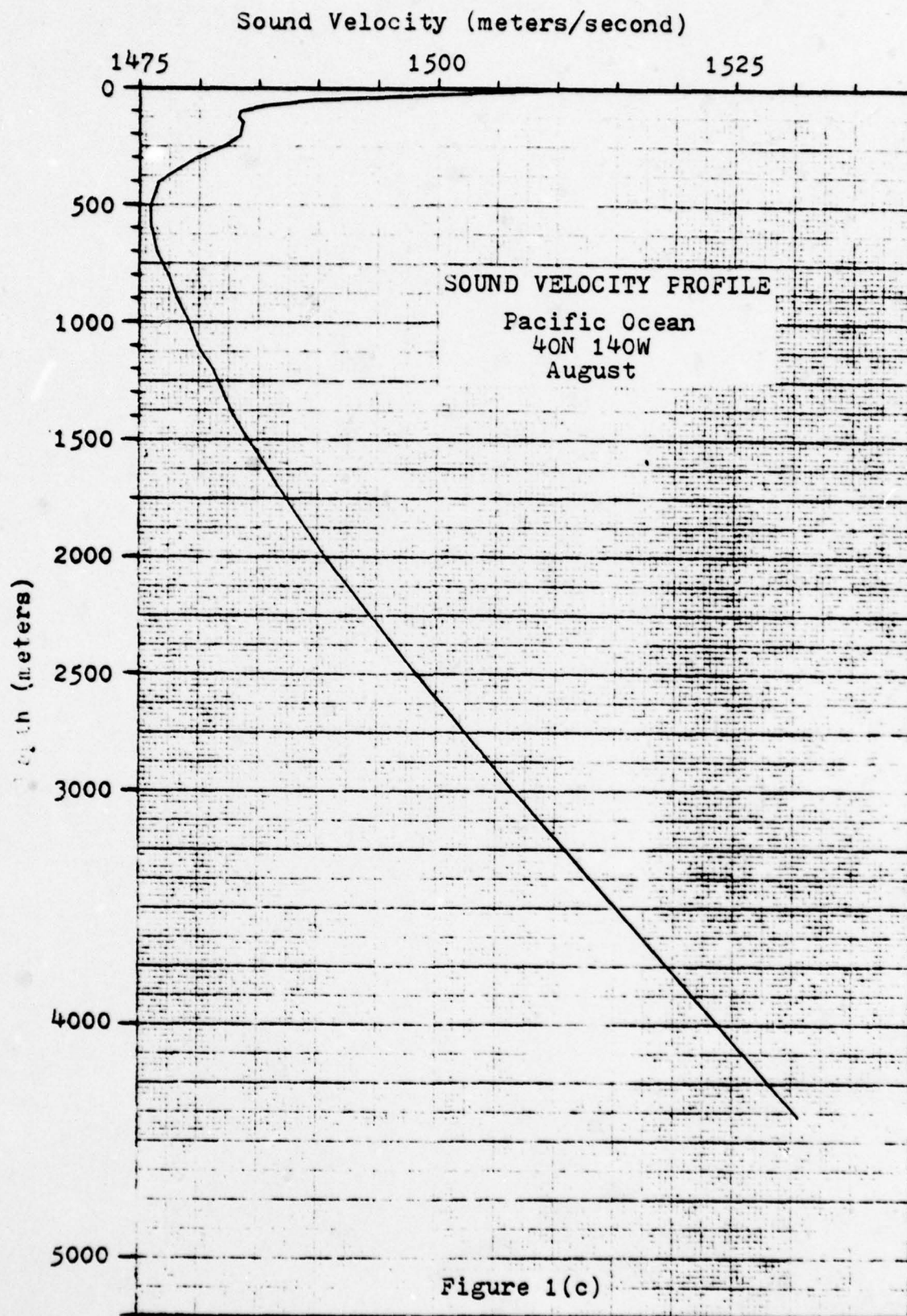
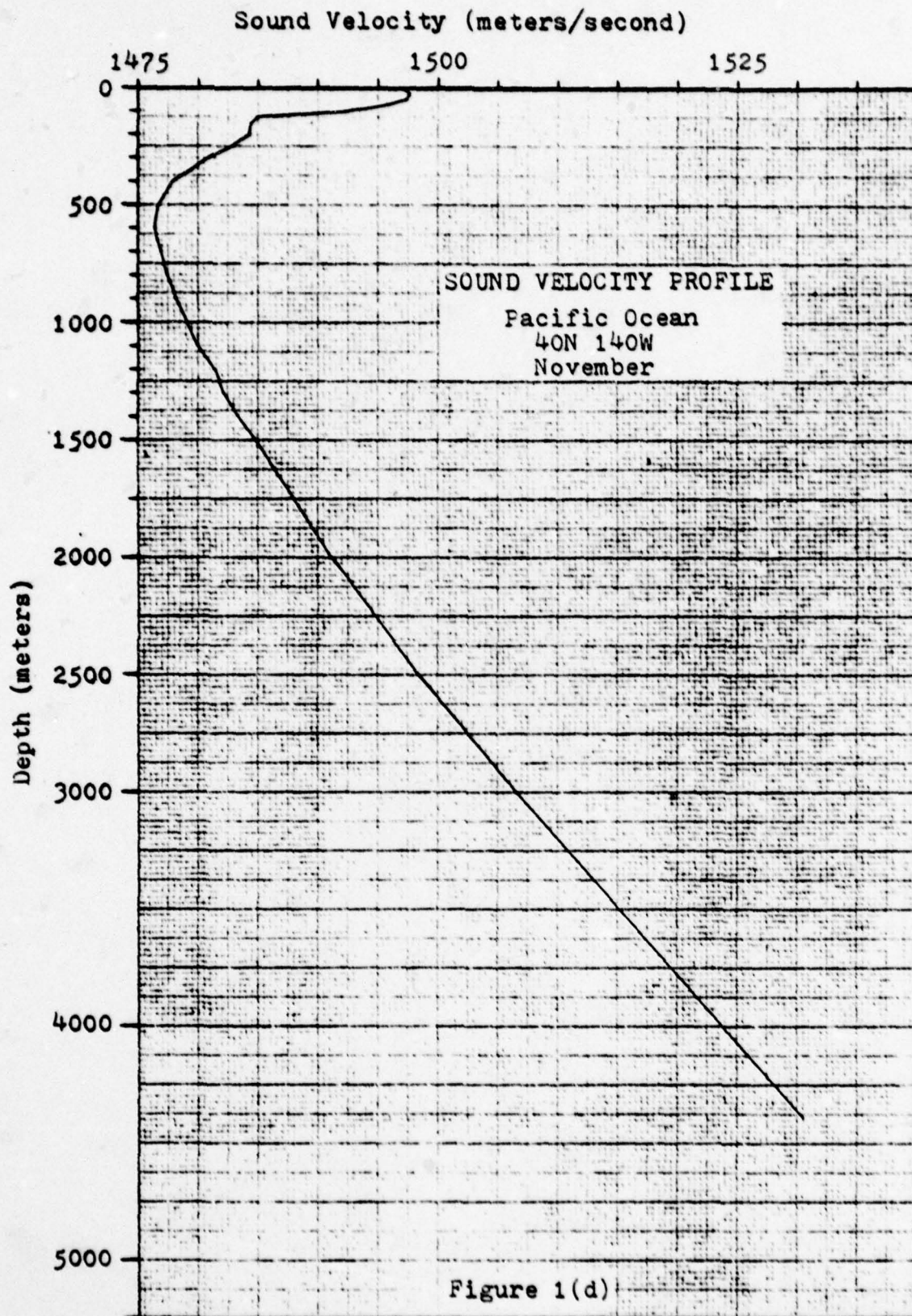
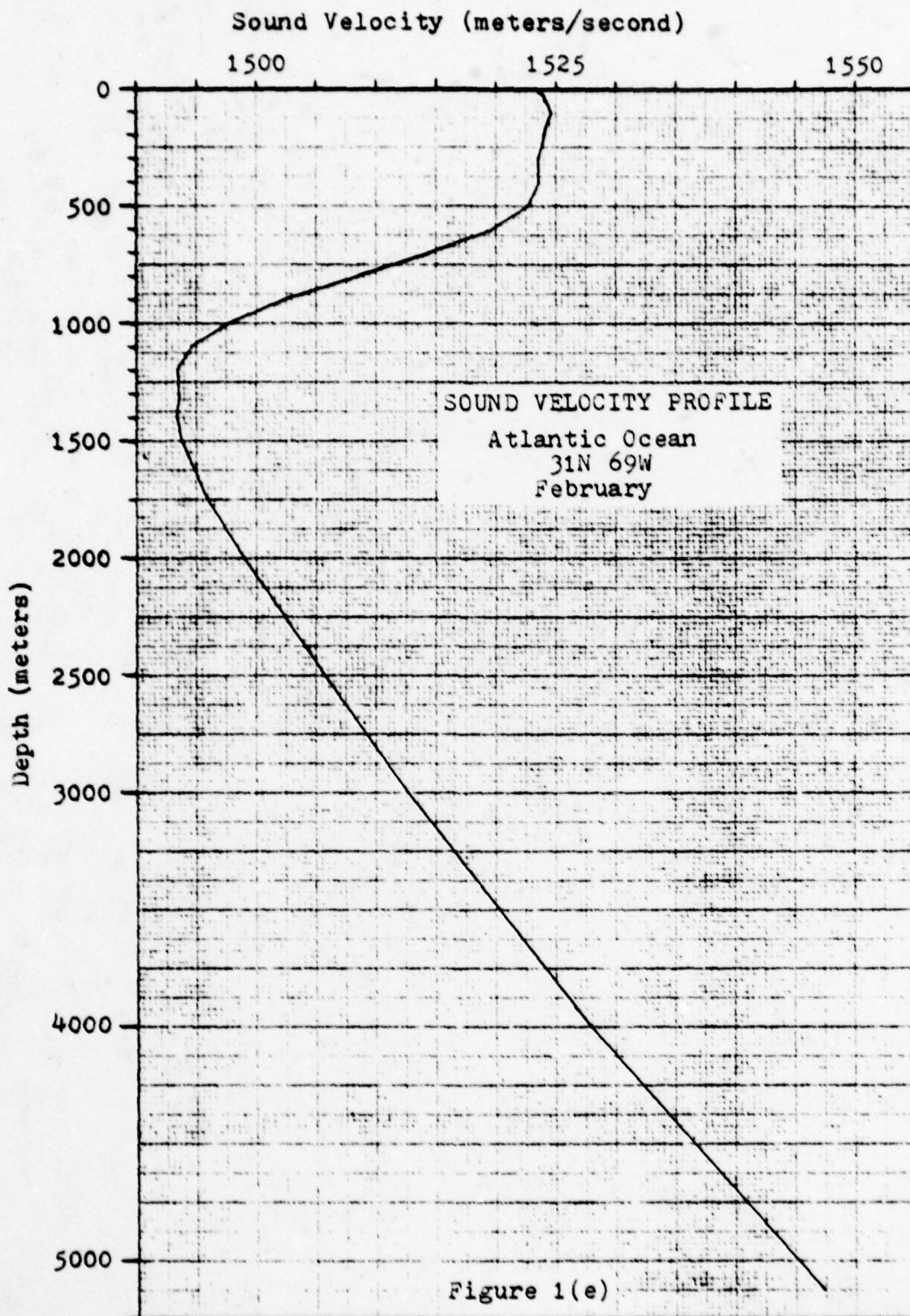


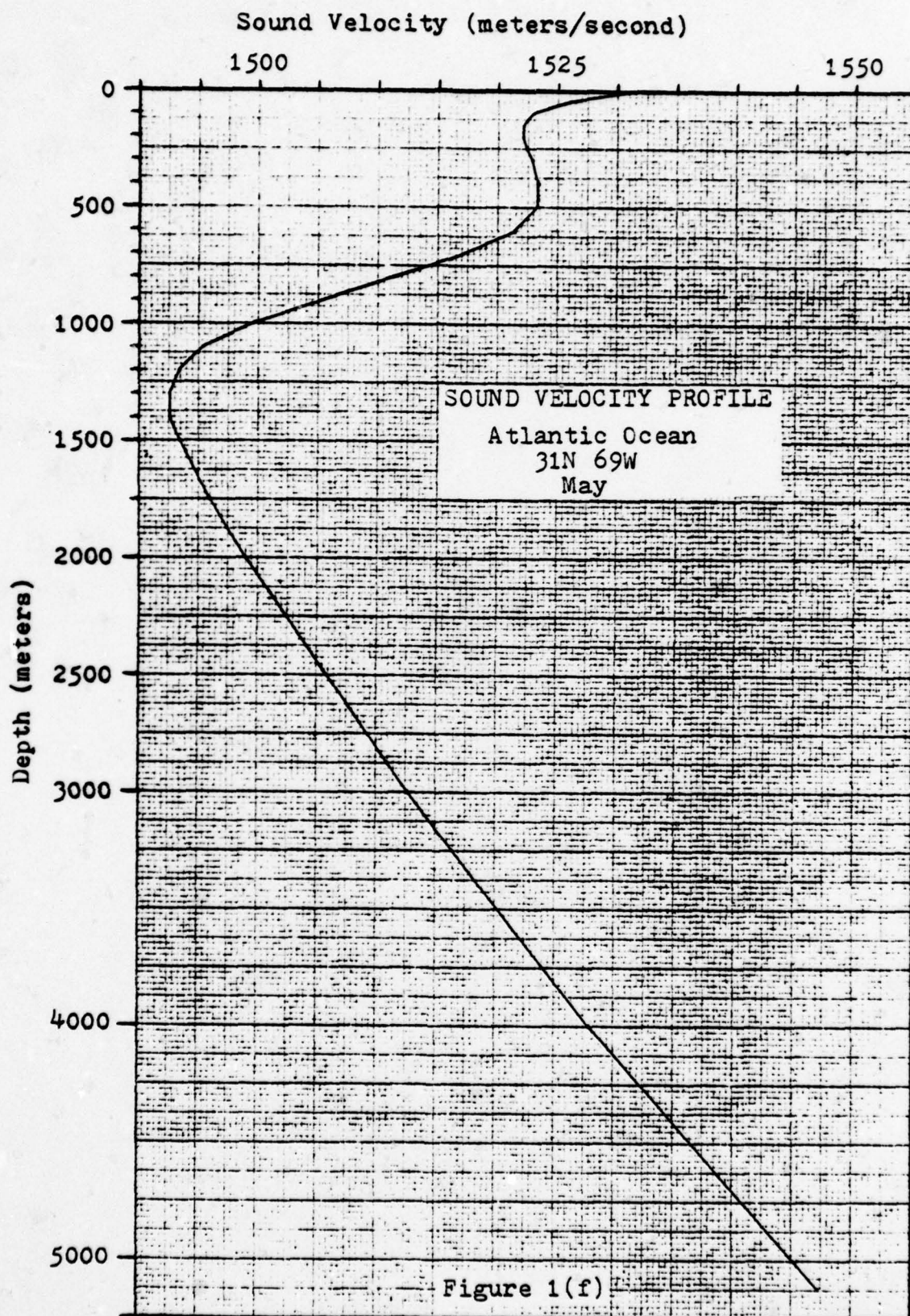
Figure 1(a)

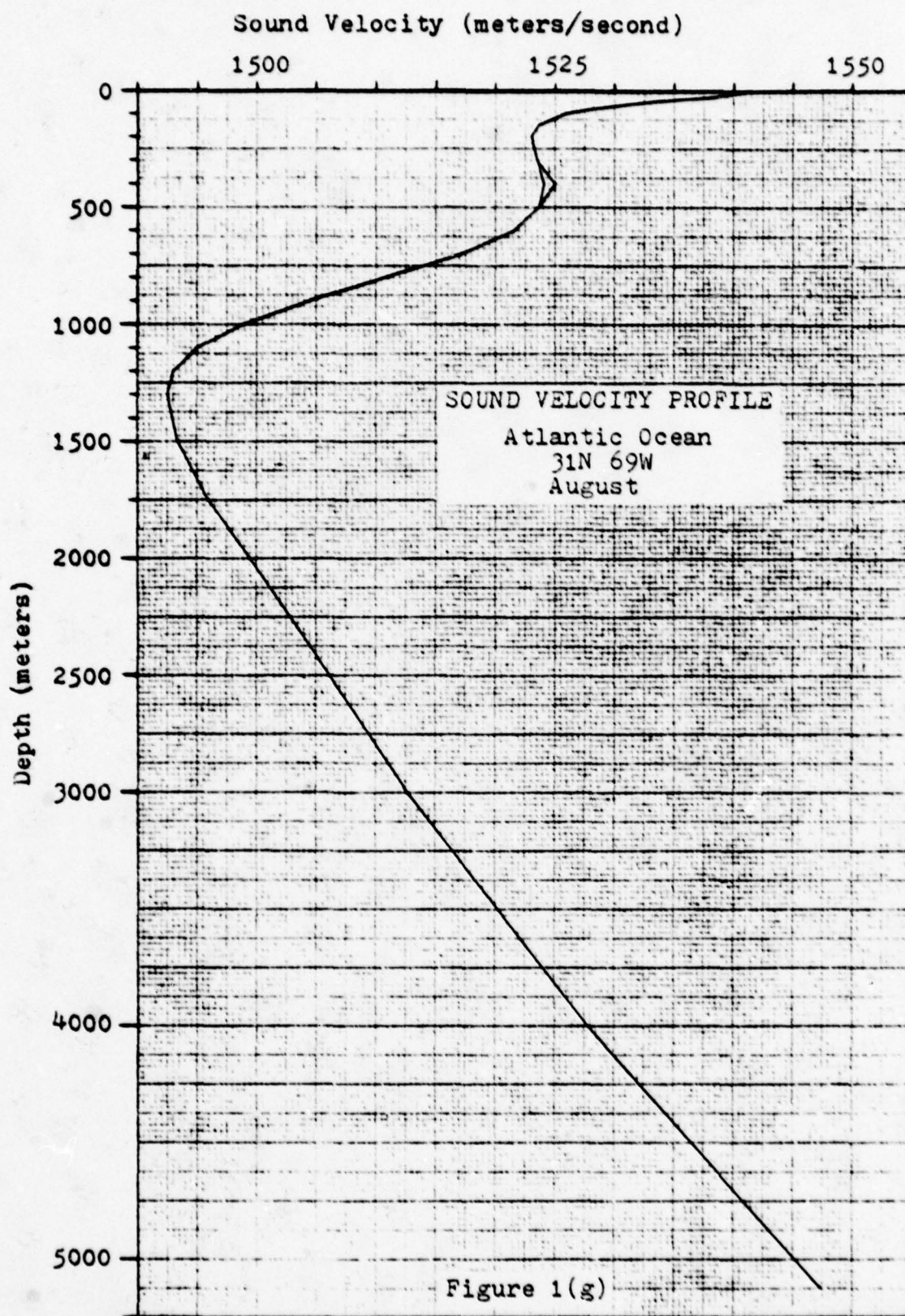


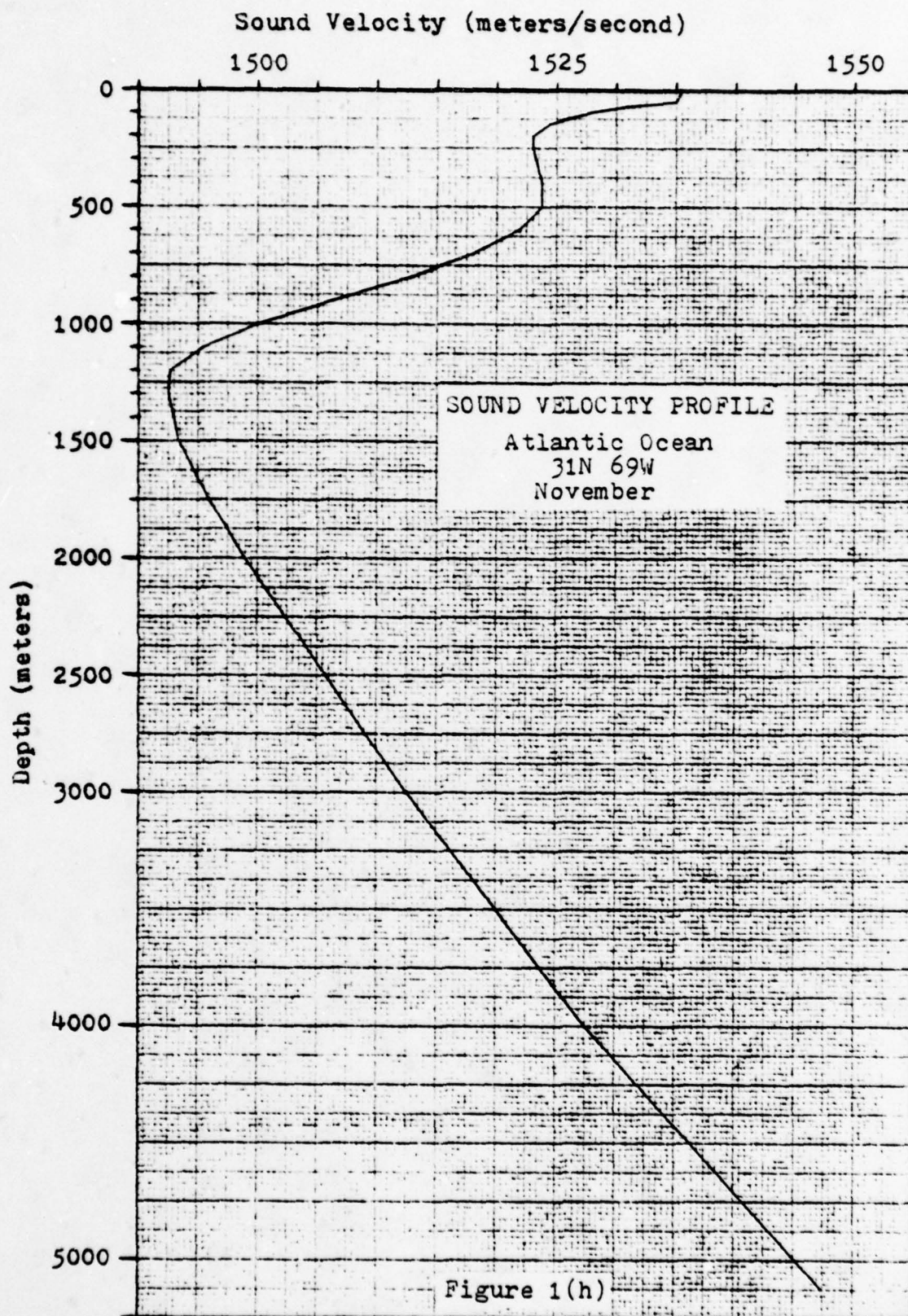


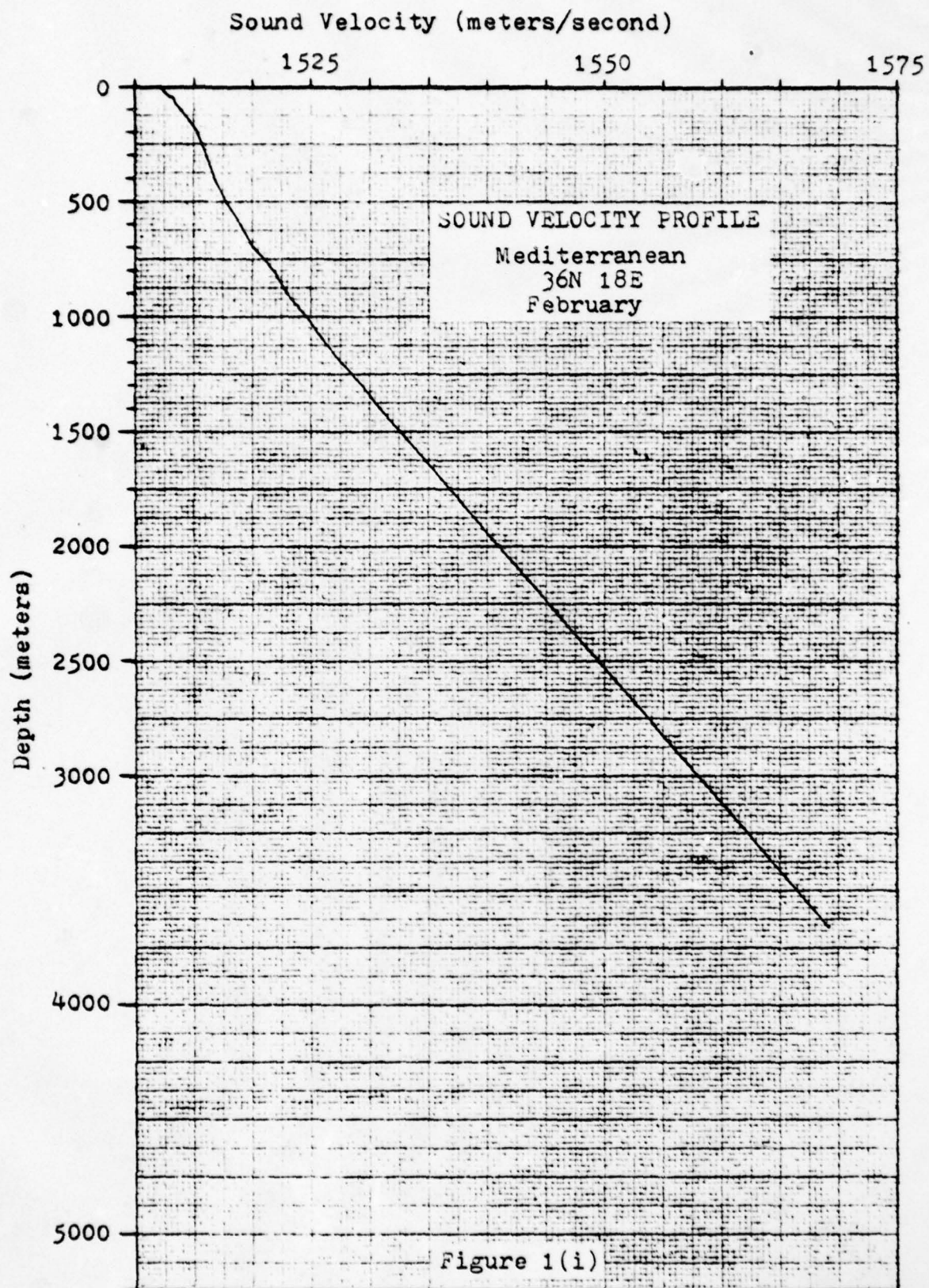


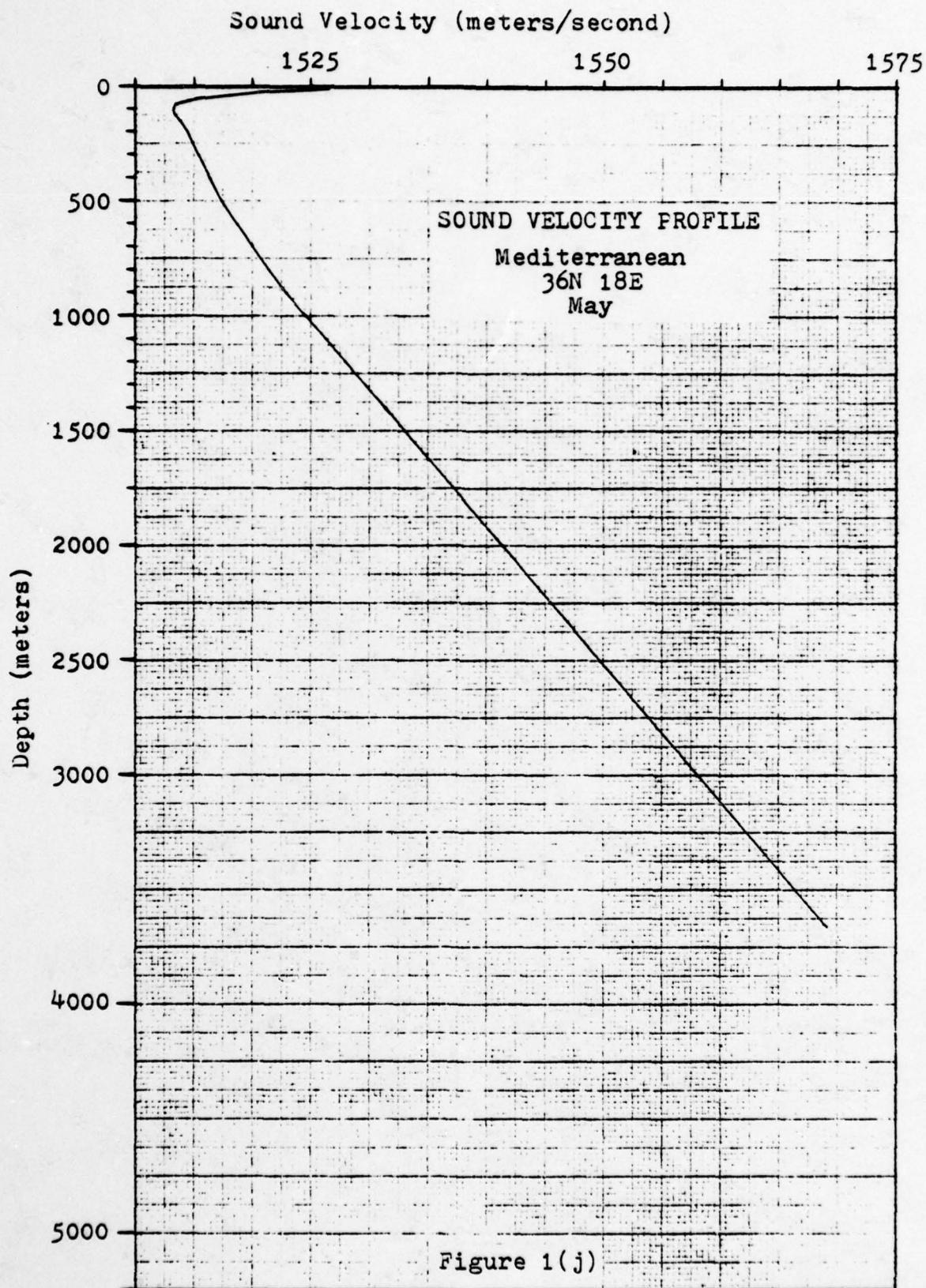


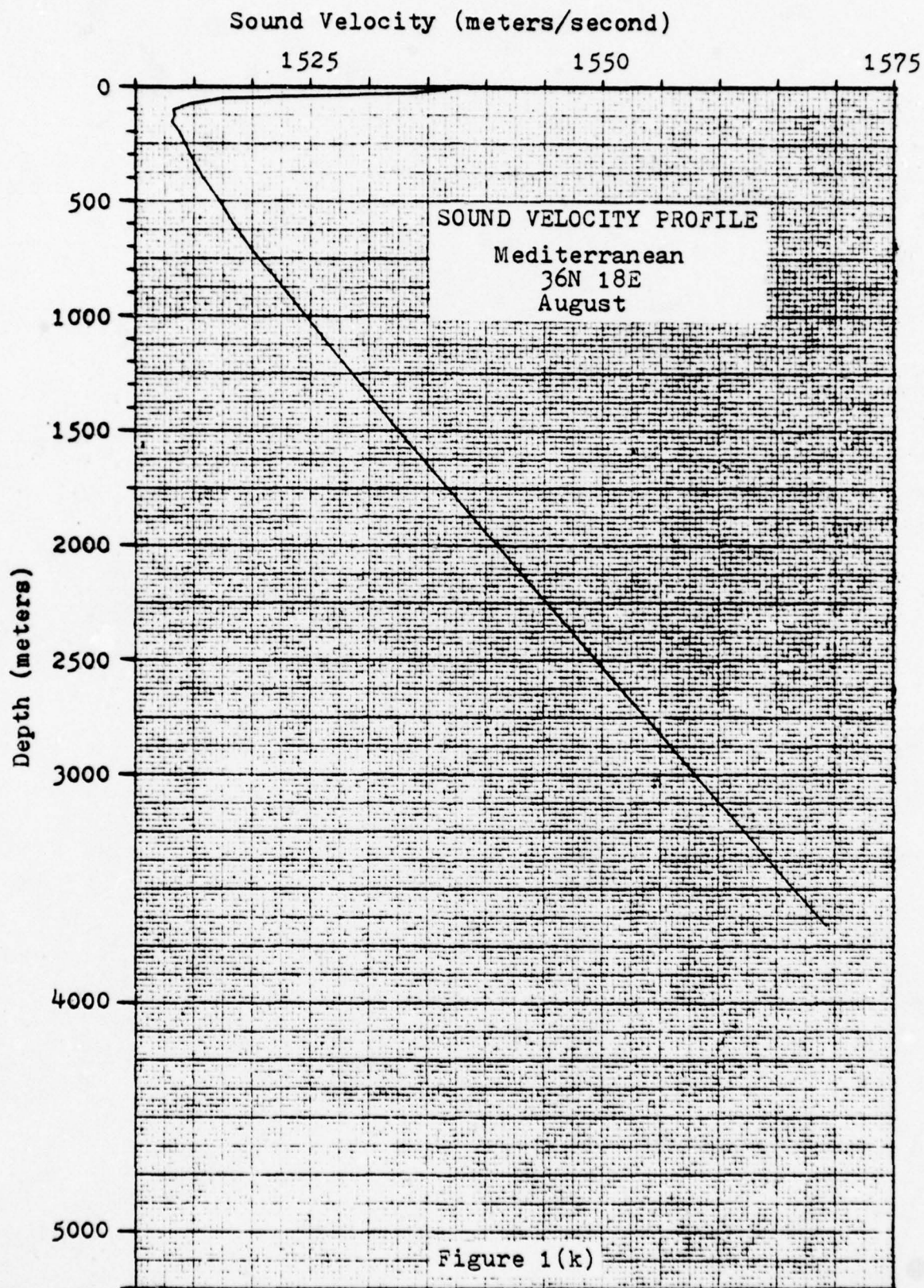


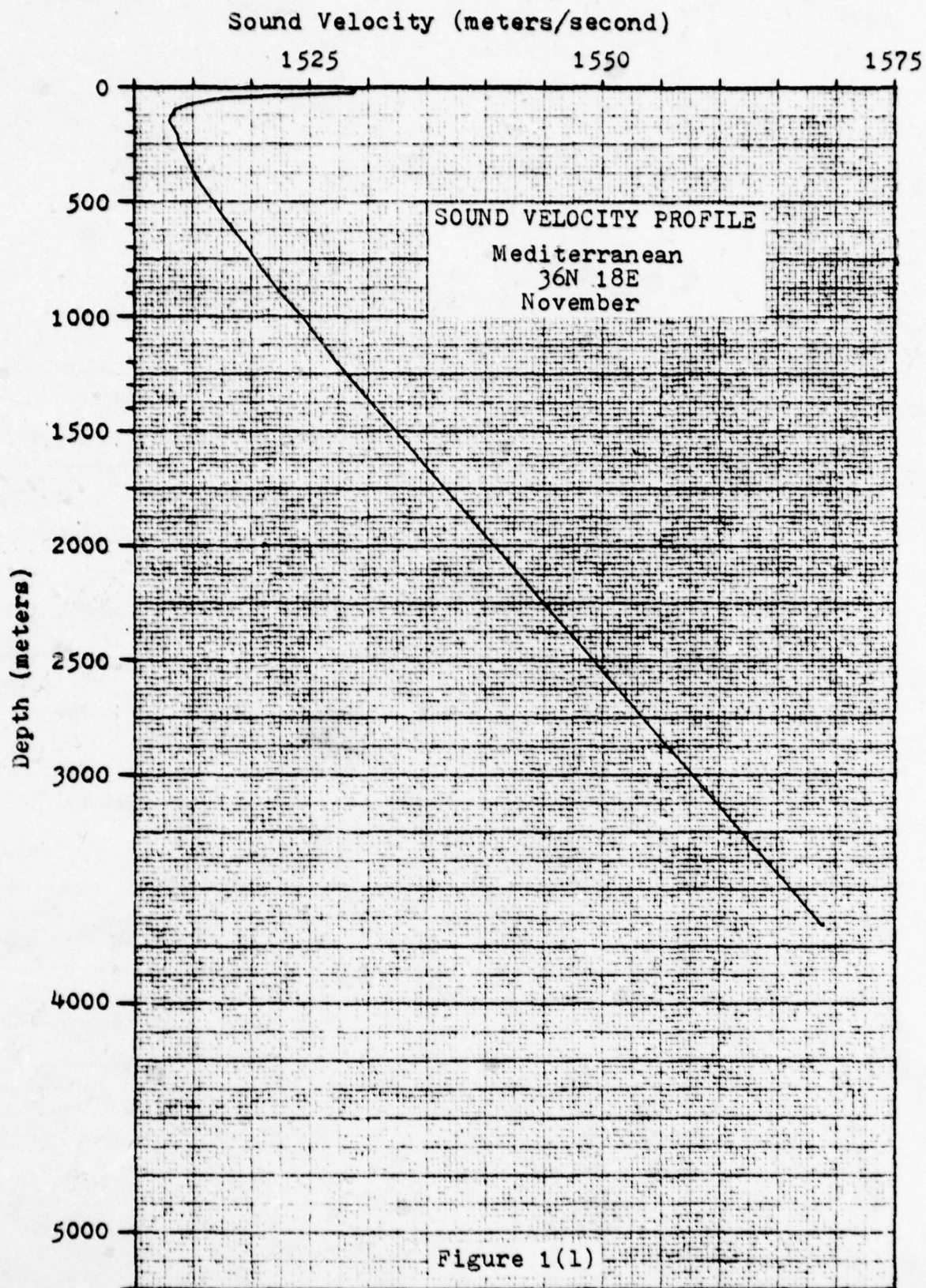












of values is for the ocean bottom depth which was part of the input data.

D. COMPARISON OF DEEP SOUND CHANNEL CHARACTERISTICS

Figure 2 depicts the deep sound channel (DSC) portion of the May SVP for the Pacific, Atlantic and Mediterranean coordinates mentioned earlier in a composite graph drawn to scale. As can be seen in that figure, DSC characteristics of the three areas differ considerably. The vertical extent of the channels varies from 1100 meters in the Mediterranean to 4200 meters in the Atlantic. The change in sound velocity between sonic layer depth (SLD) and DSC axis (point of minimum velocity) varies from 15 m/sec in the Mediterranean to 38 m/sec in the Atlantic. The depth of the DSC axis varies from 100 meters in the Mediterranean to 1300 meters in the Atlantic. Pacific Ocean values are between the others for all of those characteristics. Sound velocity near the surface is much greater in the Atlantic and Mediterranean than in the Pacific, and sound velocity near the bottom of the three basins (not shown in the figure) is about 6 m/sec greater in the Atlantic than in the Pacific and about 52 m/sec greater in the Mediterranean than in the Pacific at equal depths. Also note the subsurface sound channel located about 100 to 500 meters below the surface in the Atlantic profile.

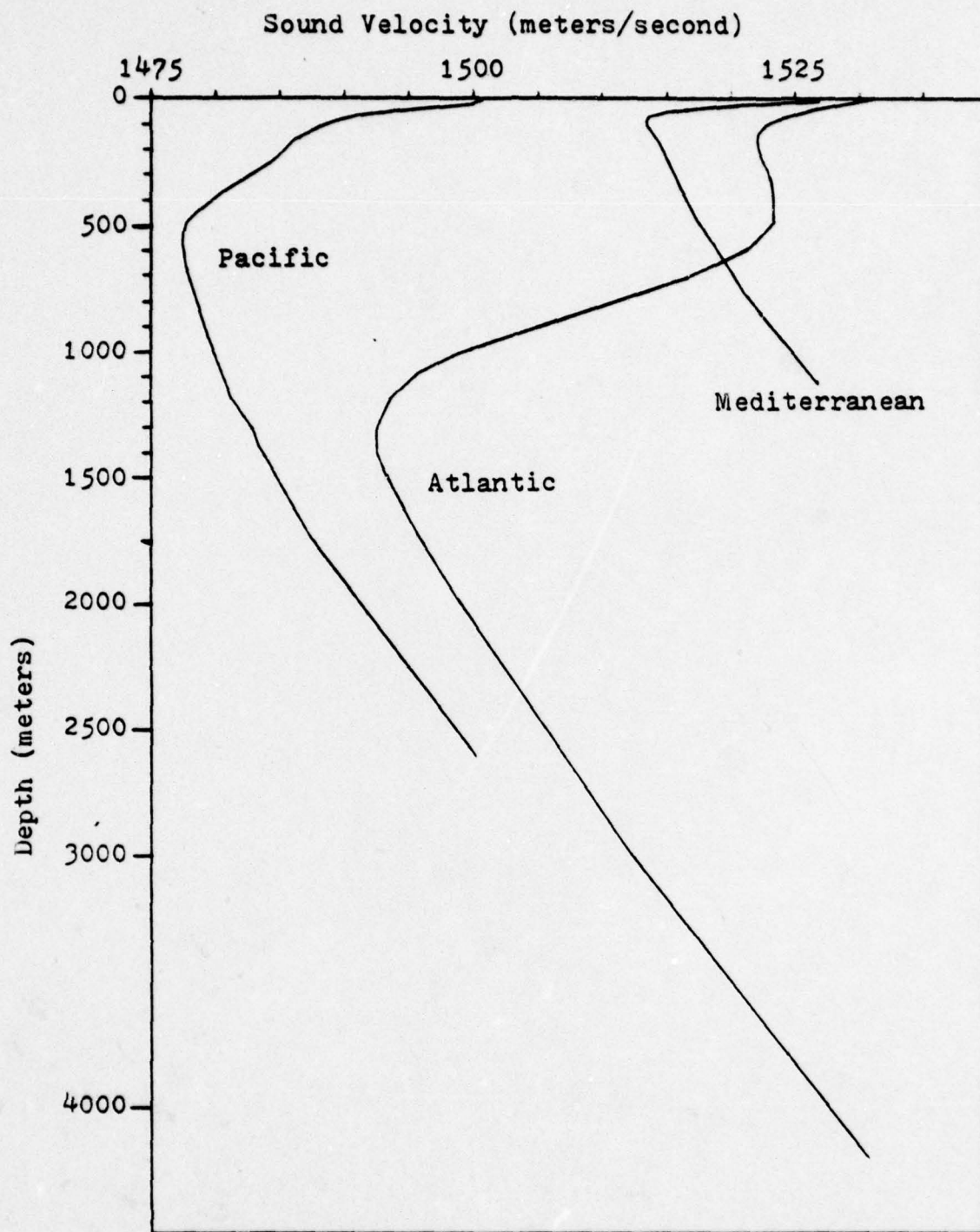


Figure 2. Comparison of Pacific, Atlantic, and Mediterranean Deep Sound Channel Characteristics.

E. COMPARISON OF CZ CHARACTERISTICS IN THREE OCEANS

1. Method Used in Obtaining Data for Comparison

There were two primary objectives in gathering twelve ICAPS runs from each of the three ocean areas. First, it was desired to obtain sufficient data to determine which CZ characteristics are common to all areas and which characteristics are peculiar to specific basins. Secondly, it was desired to obtain a standard of comparison for any calculator program which might be developed. To fulfill the first objective, it was decided to keep the input variables the same in all areas, varying them one at a time, in order to better compare the differences observed in the various runs. For each of the three locations, the inputs varied were season of the year and source and receiver depth combination. Receiver depths of 60 and 300 feet and source depths of 60 and 400 feet were used. Each of the ICAPS outputs consisted of TL profiles for four frequencies out to a range of 250 kyds.

Originally, it was intended to collect twelve data from each profile. These data were to be the range, width, CZ gain, and Transmission Loss for each of the first three convergence zone annuli. As it turned out, somewhat less data was collected and tabulated. There were several reasons for this. First, the February SVP in the Mediterranean contained no sound channel and therefore no convergence zones existed. Secondly, all of the third CZ data for the Atlantic was thrown out on the grounds that it was almost always the same and that it was inconsistent with information from

the first two CZ annuli in any particular profile. The reason for this occurrence is not know. Finally, it was impossible to obtain some of the desired data because of the smooth way in which the CZ path blended with other competitive propagation modes. One could not tell what was CZ and what was not in those cases.

2. CZ Range and Width Analysis

The transmission loss profiles produced by ICAPS are presented in two formats, a table of TL values for each kiloyard of range from the source and a graph of the same information. Because the TL values are tabulated at kiloyard intervals, it is impossible to be more accurate than that interval in determining where a CZ begins and ends. Also, it was difficult to be consistent in picking the points representing the edges of CZ annuli because of the variety of graph shapes, TL levels, and other propagation mode interferences. In any event, an attempt was made to satisfy one basic criterion in choosing leading and trailing edges of the annuli: Do these ranges best represent the apparent location of the annulus regardless of the TL levels involved? Admittedly, the ranges picked were often based on subjective judgement, and it cannot be stated with complete certainty that only CZ mode propagation contributed to the TL peaks judged to be the CZ annuli.

Table I contains the CZ range and width data that could be gleaned from the ICAPS profiles. In the table, RCZi is the range to the inner edge of the first, second, or

Table I. ICAPS CZ
Range & Width Data

Pacific 40N - 140W		1ST CZ		2ND CZ		3RD CZ	
Mo. RCVR/TGT	FREQ (Hz)	RCZ1 (Nm)	CZW (Nm) RCZO (%)	RCZ1 (Nm)	CZW (Nm) RCZO (%)	RCZ1 (Nm)	CZW (Nm) RCZO (%)
FEBRUARY							
60/60	50	25.5	5.0 16	51.0	11.0 18	77.0	16.0 17
	300	25.0	6.0 19	50.5	11.5 19	76.0	17.0 18
	850	25.5	5.5 18	51.0	10.0 16	76.5	15.5 17
	1700	25.5	5.5 18	51.0	11.0 18	76.5	16.5 18
60/400	50	25.0	6.0 19	50.0	12.5 20	76.0	17.5 19
	300	24.5	6.5 21	50.0	12.5 20	75.5	18.0 19
	850	24.5	6.5 21	50.5	11.5 19	76.0	17.5 19
	1700	24.5	6.5 21	50.5	12.0 20	76.0	17.5 19
300/400	50	24.0	7.0 23	49.0	13.5 22	74.5	19.0 20
	300	24.0	7.0 23	49.0	13.0 21	74.5	19.0 20
	850	24.0	7.0 23	49.5	13.0 21	75.0	18.5 20
	1700	24.5	6.5 21	49.5	13.0 21	75.0	18.5 20
60/60	50	26.0	4.5 15	52.0	9.5 15	78.0	14.5 16
	300	26.0	5.5 18	52.5	9.0 15	79.0	13.5 15
	850	26.5	4.0 13	53.0	8.5 14	79.5	13.0 14
	1700	26.5	4.0 13	53.0	8.5 14	79.5	13.0 14
60/400	50	25.5	5.5 18	51.0	11.0 18	78.0	14.5 16
	300	25.5	5.5 18	51.5	10.5 17	78.5	14.0 15
	850	25.5	5.5 18	52.0	10.0 16	79.0	13.5 15
	1700	25.5	5.5 18	52.0	10.0 16	78.5	14.0 15
300/400	50	24.0	7.0 23	49.0	13.0 21	74.5	18.5 20
	300	24.0	7.0 23	49.0	13.0 21	74.5	18.5 20
	850	24.0	7.0 23	49.0	12.5 20	79.0	14.0 15
	1700	24.0	7.0 23	49.0	13.0 21	74.5	18.5 20
MAY							

Table I. ICAPS CZ
Range & Width Data

Mo. RCVR/TGT FREQ (Ft)	Pacific 40W = 140W (Hz)	1ST CZ		2ND CZ		3RD CZ	
		RCZi (Nm)	CZW (Nm)	RCZi (Nm)	CZW (Nm)	RCZi (Nm)	CZW (Nm)
	50	25.0	5.5	50.0	11.0	76.5	15.0
	300	26.0	4.5	52.5	8.5	79.0	12.5
	850	26.5	4.0	53.5	7.5	80.0	11.5
	1700	26.5	4.0	53.5	7.5	80.5	11.0
	50	25.0	4.0	50.0	8.5	77.0	11.0
	300	26.0	4.0	52.0	9.0	79.0	12.5
	850	26.0	4.0	53.0	8.0	80.0	11.5
	1700	26.5	3.5	53.0	8.0	80.0	11.5
	50	23.0	5.0	46.5	10.0	70.0	12.5
	300	23.0	7.0	46.5	14.0	70.0	21.5
	850	23.5	6.5	46.5	14.0	70.5	21.0
	1700	23.5	6.5	47.0	13.5	70.5	21.0
	50	26.5	4.0	53.0	8.0	80.0	12.0
	300	26.0	4.5	52.0	9.0	78.0	14.0
	850	26.0	4.5	52.5	8.5	79.0	13.0
	1700	26.0	4.5	52.5	8.5	79.0	13.0
	50	26.0	4.5	52.0	9.5	78.5	13.5
	300	25.0	5.5	51.5	10.0	78.0	14.0
	850	25.5	5.0	52.0	9.5	78.5	13.5
	1700	25.5	5.0	52.0	9.5	78.5	13.5
	50	23.0	7.5	47.0	14.5	70.5	21.0
	300	23.5	7.5	47.5	14.0	71.5	20.5
	850	24.0	7.0	48.0	13.5	72.5	20.0
	1700	24.0	7.0	48.0	13.5	72.5	19.5

AUGUST

NOVEMBER

Table I. ICAPS CZ
Range & Width Data

Atlantic 3IN - 69W		1ST CZ		2ND CZ		3RD CZ	
Mo. RCVR/TGT	FREQ (Hz)	RCZi (Nm)	CZW (Nm) RCZo (%)	RCZi (Nm)	CZW (Nm) RCZo (%)	RCZi (Nm)	CZW (Nm) RCZo (%)
FEBRUARY							
60/60	50	34.0	3.0 8	68.5	-		
	300	35.0	-	70.0	-		
	850	35.0	4.0 10	69.5	10.0 13		
	1700	35.5	5.5 13	69.5	9.0 12		
60/400	50	34.0	3.5 9	68.5	6.5 9		
	300	34.5	10.5 23	69.5	21.0 23		
	850	34.5	6.5 16	69.5	8.5 11		
	1700	34.5	3.5 9	69.5	11.0 14		
300/400	50	34.0	8.0 19	68.0	-		
	300	34.0	-	69.0	-		
	850	34.0	-	69.0	-		
	1700	34.0	-	69.0	-		
60/60	50	34.5	5.5 14	69.0	11.5 14		
	300	34.5	3.5 9	69.0	8.0 10		
	850	35.0	2.5 7	69.5	6.0 8		
	1700	35.0	2.5 7	69.5	5.5 7		
60/400	50	34.0	4.0 11	69.0	8.0 10		
	300	34.5	4.0 10	69.0	6.5 9		
	850	34.5	3.5 9	69.5	6.0 8		
	1700	34.5	3.5 9	69.5	6.0 8		
300/400	50	33.5	2.0 6	68.5	2.5 4		
	300	34.0	7.0 17	69.0	-		
	850	34.0	5.5 14	69.0	7.5 10		
	1700	34.0	5.0 13	69.0	6.0 8		
MAY							

Table I. ICAPS CZ
Range & Width Data

Atlantic 31N - 69W		1ST CZ		2ND CZ		3RD CZ	
Mo. RCVR/TGT	FREQ (Hz)	RCZi (Nm)	CZW (Nm)	RCZO (%)	RCZi (Nm)	CZW (Nm)	RCZO (%)
60/60		33.0	4.0	11	66.5	7.0	10
300		35.0	2.0	5	70.0	3.5	5
850		35.0	2.0	5	70.5	3.0	4
1700		35.5	1.5	4	71.0	2.5	3
60/400		34.5	3.5	9	68.0	5.0	7
300		34.5	3.5	9	69.5	4.5	6
850		34.5	3.5	9	70.0	4.0	5
1700		35.0	3.0	8	70.5	3.5	5
60/60		34.0	6.5	16	69.5	10.5	13
300		34.0	6.0	15	69.5	10.5	13
850		34.5	5.5	14	70.0	8.5	11
1700		34.5	5.0	13	70.0	8.0	10
60/60		34.5	1.5	4	69.5	2.5	4
300		35.0	4.5	11	70.0	9.0	11
850		35.0	4.5	11	70.0	9.0	11
1700		35.0	4.5	11	70.0	9.0	11
60/400		34.0	3.5	9	69.0	3.0	4
300		34.5	4.0	10	69.5	7.5	10
850		34.5	5.0	13	69.5	10.0	13
1700		34.5	6.0	15	70.0	10.0	13
60/60		34.0	6.0	15	69.0	11.0	14
300		34.0	5.5	14	69.5	8.5	11
850		34.0	4.5	12	69.5	6.5	9
1700		34.5	4.0	10	69.5	6.0	8

AUGUST

NOVEMBER

Table I. ICAPS CZ
Range & Width Data
Mediterranean
36N - 18E

Mo. RCVR/TGT (Ft)	FREQ (Hz)	1ST CZ		2ND CZ		3RD CZ	
		RCZi (Nm)	CZW (Nm)	RCZi (Nm)	CZW (Nm)	RCZi (Nm)	CZW (Nm)
60/60	50	NONE					
	300	NONE					
	850	NONE					
	1700	NONE					
60/400	50	NONE					
	300	NONE					
	850	NONE					
	1700	NONE					
300/400	50	NONE					
	300	NONE					
	850	NONE					
	1700	NONE					
60/60	50	15.0	2.0	30.5	2.0	46.5	2.5
	300	14.5	4.0	29.5	9.5	45.0	11.5
	850	15.0	2.5	30.5	2.0	45.5	3.5
	1700	15.0	2.0	30.5	2.0	46.0	3.0
60/400	50	14.5	0.5	30.5	1.0	42.0	4.0
	300	15.0	2.5	30.0	3.0	45.0	4.5
	850	14.5	2.5	30.0	3.0	44.5	4.5
	1700	14.5	2.5	30.0	3.0	45.5	3.0
300/400	50	14.5	2.0	30.5	2.5	45.5	3.5
	300	15.5	0.5	31.0	1.0	47.0	1.5
	850	14.5	1.5	30.5	1.0	45.5	3.0
	1700	14.5	1.5	30.5	2.0	45.5	3.0

FEBRUARY

MAY

Table I. ICAPS CZ
Range & Width Data
Mediterranean
36N-18E

Mo.	RCVR/TGT (Ft)	FREQ (Hz)	1ST CZ		2ND CZ		3RD CZ	
			RCZI (Nm)	CZW (Nm)	RCZI (Nm)	CZW (Nm)	RCZI (Nm)	CZW (Nm)
AUGUST	60/60	50	18.0	1.5	37.0	1.5	52.0	6.0
		300	18.0	3.0	36.5	2.0	52.5	5.5
		850	18.0	2.0	36.5	2.0	54.5	3.5
		1700	18.0	2.0	36.5	2.0	54.5	3.5
	60/400	50	18.0	2.0	36.5	1.5	53.5	4.5
		300	17.5	3.0	36.0	3.0	53.5	5.0
		850	18.0	3.5	36.5	2.5	54.0	4.5
		1700	17.5	2.5	36.0	3.0	54.5	4.0
	300/400	50	NONE					
		300	NONE					
		850	NONE					
		1700	NONE					
NOVEMBER	60/60	50	16.5	3.5	36.0	5.0	54.0	7.0
		300	16.0	2.5	35.0	1.5	53.0	5.0
		850	16.5	3.0	35.5	2.0	53.5	5.0
		1700	16.5	3.0	35.5	3.0	53.5	4.5
	60/400	50	17.0	3.5	36.0	4.0	52.0	7.0
		300	17.0	2.5	35.5	3.5	53.5	4.5
		850	17.0	3.0	35.0	5.0	53.5	5.0
		1700	17.0	2.5	35.0	4.5	53.5	3.0
	300/400	50	10.0	2.5	20.5	3.5	31.5	5.0
		300	9.5	3.0	20.0	4.5	31.0	5.5
		850	9.5	3.0	20.0	3.5	30.5	3.5
		1700	9.5	2.0	20.0	2.5	30.5	2.5

third CZ annulus to the nearest one half nautical mile. CZW is the width of the annulus also the nearest one half nautical mile. The third column of numbers is the ratio of CZW to the range of the outer edge of the annulus (RCZo), expressed as a percentage.

After carefully studying this data, the following conclusions were made concerning CZ propagation:

(1) The range to the first CZ is approximately 14 to 18 nm at the Mediterranean location, 23 to 27 nm at the Pacific location, and 33 to 35 nm at the Atlantic location.

(2) Range to the CZ decreases and annulus width increases as source and receiver get deeper in all cases.

(3) The ranges to the second and third annuli are approximately whole number multiples of the ranges to the inner and outer edges of the first annulus in all cases.

(4) The range or width of a CZ annulus does not appear to have any significant frequency dependence.

3. CZ Gain and Transmission Loss Analysis

Convergence zone gain is defined as the difference between the transmission loss expected under conditions of spherical propagation and the actual transmission loss observed. This definition is expressed in Eq. (1).

$$G = 20 \log(r) + a(r) - TL \quad (1)$$

In this equation, G is the CZ gain, r is the range to the

CZ annulus, α is the attenuation coefficient associated with the frequency of interest, and TL is the actual transmission loss observed in the CZ annulus for that frequency. All terms in Eq. (1) are in decibels (dB).

In actual convergence zones, TL (and therefore gain) is by no means a constant value. Contributions of several possible propagation paths at any one point and the time varying nature of sound paths in the ocean cause coherence effects to exist. These effects make TL vary in both space and time. Coherence effects are more pronounced at lower frequencies (longer wavelengths) where the time varying effects are small compared to spatially distributed effects. In ICAPS, the more predictable coherence conditions are included in the mathematical model.

Since a single TL value was desired for the envisioned calculator model, an attempt was made to pick the "average" TL in the ICAPS CZ annuli. As with the range estimates, this called for subjective judgement. Figure 3 shows a typical ICAPS CZ presentation which has coherence effects in evidence. The figure suggests how an "average" TL was chosen as best representing that annulus. Two levels were chosen (labeled high and low in the figure) which bracket the majority of the TL points within the annulus. The approximate midpoint between those levels was then picked as "the" TL for that CZ.

As an extra point of interest, the high and low TL levels were studied. It was noted that ICAPS predicts TL

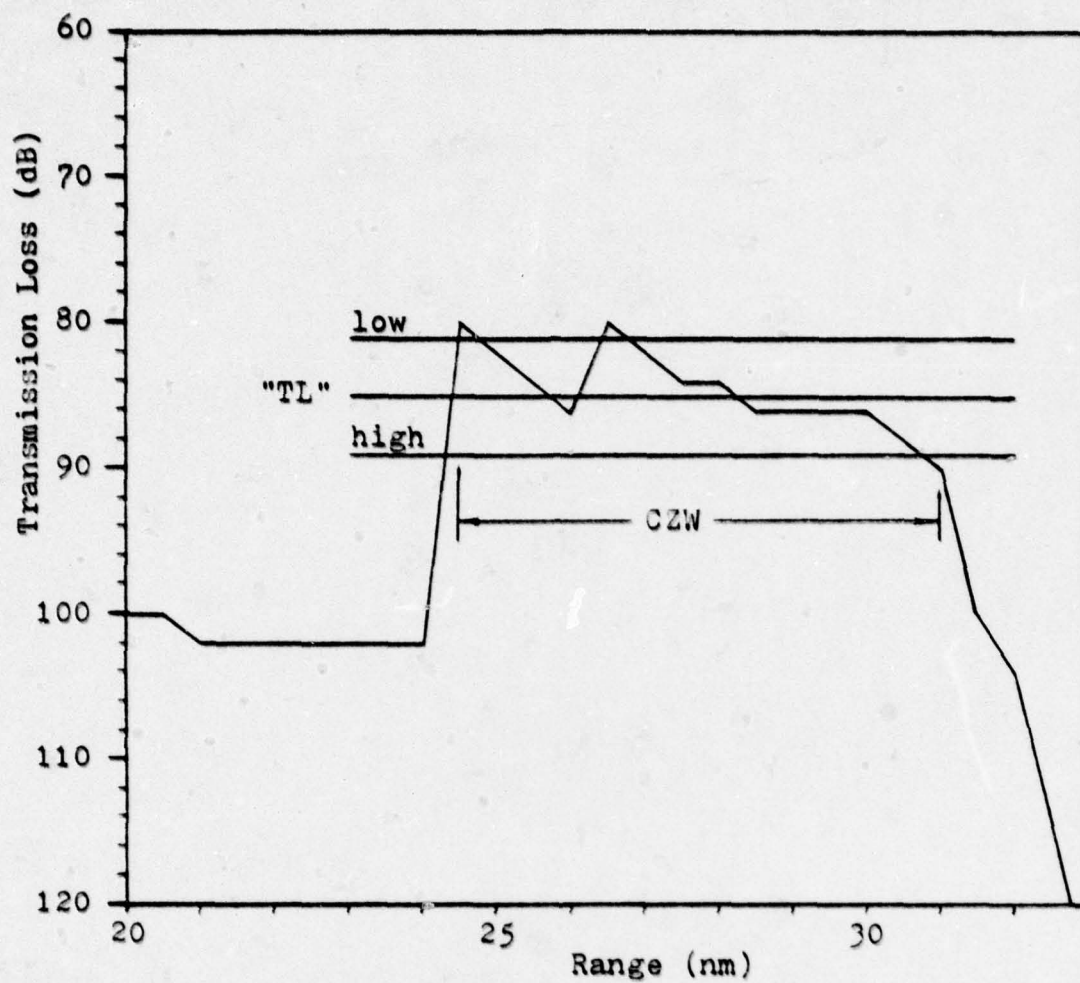


Figure 3. Estimating Transmission Loss in a CZ Annulus from an ICAPS TL Profile.

variations from about ± 10 dB around the "average" level. If this is truly representative of CZ coherence effects, an ASW unit armed only with an estimate of the "average" TL in a certain CZ annulus should expect to see variations of about that magnitude around the estimate in hand.

Using TL levels estimated by the procedure described above, and employing Eq. (1), CZ gain values predicted by ICAPS were obtained and tabulated. The values produced are contained in Tables II and III. Table II shows all of the data from the Pacific location. Table III contains only 300 Hz data from the Atlantic and Mediterranean locations. (50, 850, and 1700 Hz data were omitted from Table III because it became obvious during data collection that G is not frequency dependent.)

Again after careful study, the following conclusions were drawn concerning CZ gain:

- (1) CZ gain values range from about eight to twenty dB in all three areas observed.

- (2) CZ gain is the same value for first, second, and third CZ in any given case.

- (3) In general, CZ gain is independent of frequency. An exception to this conclusion is that at low frequency (below 300 Hz), especially when source or receiver or both are above the SLD and/or near the surface, there is apparently somewhat less gain than evident for higher frequencies. This difference is probably due to stronger diffraction of the longer wavelengths.

(4) CZ gain seems to be highest when source and receiver are at or near the same depth.

<u>Month</u> <u>SLD(ft)</u>	<u>Rcvr/Tgt</u> <u>(ft)</u>	<u>Freq</u> <u>(Hz)</u>	<u>1st CZ</u>	<u>CZ Gain (dB)</u> <u>2nd CZ</u>	<u>3rd CZ</u>
<u>FEB</u> <u>246</u>	60/60	50	7	7	6
		300	14	13	12
		850	14	13	13
		1700	15	15	12
	60/400	50	9	9	9
		300	12	12	11
		850	11	11	12
		1700	11	11	12
	300/400	50	12	11	10
		300	12	12	11
		850	10	11	12
		1700	12	10	11
<u>MAY</u> <u>33</u>	60/60	50	16	17	16
		300	16	17	16
		850	16	17	16
		1700	16	17	17
	60/400	50	10	10	12
		300	10	11	13
		850	11	12	15
		1700	9	11	12
	300/400	50	14	14	14
		300	13	13	14
		850	13	14	11
		1700	12	11	13

Table II. ICAPS CZ Gain Data Observed at the Pacific Ocean Location. (Page 1 of 2)

<u>Month</u> <u>SLD(ft)</u>	<u>Rcvr/Tgt</u> <u>(ft)</u>	<u>Freq</u> <u>(Hz)</u>	<u>1st CZ</u>	<u>CZ Gain (dB)</u> <u>2nd CZ</u>	<u>3rd CZ</u>
<u>AUG</u> <u>0</u>	60/60	50	11	11	13
		300	14	13	12
		850	15	18	20
		1700	16	17	18
	60/400	50	7	7	8
		300	9	12	13
		850	12	14	15
		1700	12	13	15
	300/400	50	14	14	14
		300	11	14	12
		850	11	12	15
		1700	12	13	11
<u>NOV</u> <u>98</u>	60/60	50	8	7	6
		300	9	12	12
		850	15	18	16
		1700	14	15	15
	60/400	50	9	9	8
		300	12	13	11
		850	11	11	11
		1700	11	11	11
	300/400	50	11	11	11
		300	12	11	11
		850	9	11	12
		1700	10	9	11

Table II. ICAPS CZ Gain Data Observed at the Pacific Ocean Location. (Page 2 of 2)

Ocean	Month SLD(ft)	Rcvr/Tgt (ft)	300 Hz CZ Gain		
			1st CZ	2nd CZ	3rd CZ
<u>ATLANTIC</u>	<u>FEB</u> 328	60/60	17	14	
		60/400	13	13	
		300/400	17	18	
	<u>MAY</u> 0	60/60	19	14	
		60/400	16	12	
		300/400	13	17	
	<u>AUG</u> 0	60/60	15	17	
		60/400	10	13	
		300/400	14	15	
	<u>NOV</u> 0	60/90	13	11	
		60/400	12	10	
		300/400	13	12	
<u>MEDITERRANEAN</u>	<u>MAY</u> 10	60/60	14	13	16
		60/400	12	10	10
		300/400	17	18	20
	<u>AUG</u> 0	60/60	17	19	17
		60/400	11	9	10
		300/400			
	<u>NOV</u> 10	60/60	11	13	15
		60/400	10	11	12
		300/400	12	14	15

Table III. ICAPS 300Hz CZ Gain Data Observed at Atlantic and Mediterranean Locations.

III. CZ RAY THEORY ANALYSIS AND MODEL DEVELOPMENT

A. CZ RANGE AND WIDTH

It was decided to use ray tracing as the method for determining CZ range and width because of the simplicity of the mathematics involved and because of the intuitive appeal of sound rays depicting the propagation of sound. The alternative approach, that of normal mode theory, was rejected on the grounds that it would be much more complicated, requiring capabilities far beyond those available in the calculators at hand.

Figure 4 shows four sound rays of particular interest in CZ propagation. The order of these rays is described for the "typical" case in the following discussion. An "atypical" case will be mentioned later.

Ray #1 departs the SLD at zero degree depression angle. It reaches its greatest depth at the bottom of the DSC and returns to the SLD at some particular range and at horizontal incidence. The horizontal range from SLD to SLD is termed cycle distance. The cycle distance for this ray is designated r_0 .

Ray #2 is the next ray of interest found as the departure angle from the SLD is increased downward. This ray passes down through and below the bottom of the DSC before turning back upward. It returns to the SLD at the shortest range from the starting point of any ray within the bundle of rays

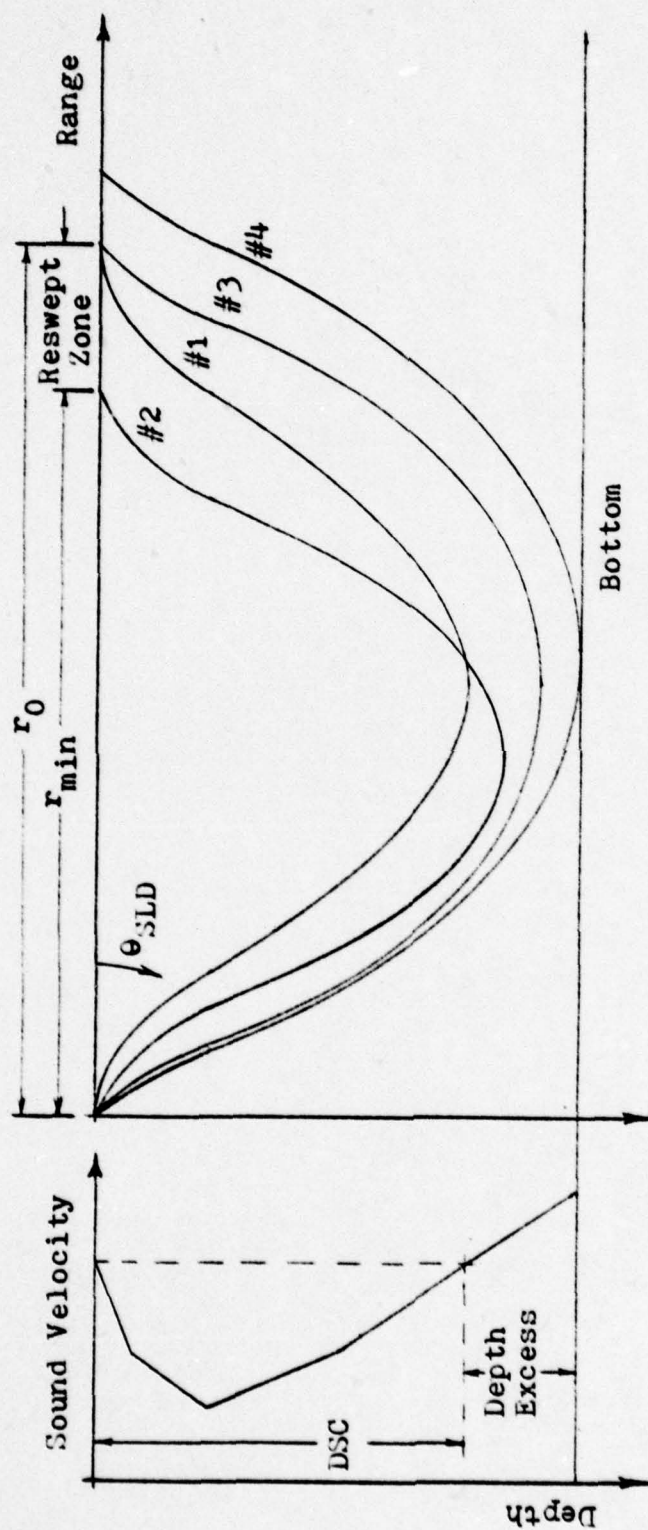


Figure 4. Sound Rays of Interest in CZ Propagation

undergoing CZ refraction. This range is designated r_{\min} . The angle of departure for this ray is designated $\theta_{r\min}$. Each ray between #1 and #2 crosses all of the previous (lesser departure angle) rays on its way up from its lowest depth.

As departure angle from the SLD is further increased, the next sound ray of interest, #3, is located. This ray has a cycle distance equal to r_0 . Its maximum depth is greater than that for ray #2. It departs from and arrives back at the SLD at an angle designated θ_{rswp} . Rays between #2 and #3 do not cross each other, but they do cross the earlier rays on their way back up to the SLD.

In the CZ annulus, the rays between #1 and #2 sweep inward toward the source as departure angle increases. After ray #2 they sweep out away from the source as angle increases further. For this reason, the region formed by rays between #1 and #3 is called the reswept zone.

Finally, as angle of departure from the SLD is increased to maximum angle for CZ propagation, we observe ray #4. This ray turns upward at a depth equal to the water column depth at that location. It returns to the SLD at the greatest distance of all CZ refracted rays. Rays departing the SLD at angles greater than that for ray #4 would be reflected off the bottom and are not of significance for the CZ propagation path.

As mentioned earlier, this progression of rays exists in a "typical" CZ situation. If, however, the ocean bottom

were more shallow, cycle distance for ray #4 would be reduced. If the bottom were shallow enough, ray #4's cycle distance would be less than r_0 . In that case, the reswept zone would be reduced to the region between rays #2 and #4. This situation is called the "atypical" case.

B. RANGE AND WIDTH MODEL

In the calculator programs developed, provision is made for entering and storing a five point sound velocity profile which defines the DSC only. The first depth and velocity pair entered (D_1, C_1) equate to the appropriate values found at the SLD. The fifth depth entered (D_5) is the depth at the bottom of the DSC where sound velocity is equal to that at the SLD. The other three depth/velocity pairs must be picked subjectively from a graph of the SVP of interest. If a mixed layer exists, the gradient in that layer is taken to be 0.02 sec^{-1} (a purely pressure induced gradient to two place accuracy). The program calculates the four layer gradients within the DSC profile entered, and uses the fourth (deepest) layer gradient in ray calculations that occur below the DSC. It would have been desirable to allow several more points in the SVP, but calculator data storage capacity and program step limitations preclude more than five depth/velocity pairs.

The overall scheme used to predict CZ range and width is to trace a series of rays starting at the SLD with a zero depression angle ray. That first ray yields r_0 which is stored.

Then an iterative process is begun in which the angle is incremented and each succeeding cycle distance determined is compared to the previous one until r_{\min} and θ_{\min} are found. (θ_{\min} is stored for use in the CZ gain and TL program, to be discussed later.) Corrections are then made to r_{\min} and r_0 to account for surface duct effects (if any) and source and receiver depth separation from the SLD. Range to the inner edge of the CZ is r_{\min} plus corrections, and range to the outer edge is r_0 plus corrections.

In the first attempt to produce a calculator program, the cycle distance of ray #4 (the ray just grazing the bottom) was compared to r_0 . The greater of the two was picked as the basic distance for determining range to the outer edge of a CZ. Later on, this portion of the program had to be deleted to save program steps. The final programs developed ignore bottom depth and do not include rays outside the reswept zone in determining annular width. This is probably a shortcoming of the programs but the seriousness of the errors it causes will not be known without further study.

A commonly applied rule-of-thumb states there must be a minimum 300 fathoms of depth excess (water column below the DSC) in order to have "reliable" CZ conditions. It was observed that a fully developed reswept zone existed in every case in the locations studied, and separate calculations showed that somewhat less than 300 fathoms depth excess was required to complete the zone. Therefore, a program user should consider the 300 fathom rule-of-thumb before

running the range and width program. With less than 300 fathoms depth excess, the possibility exists for an "atypical" CZ propagation situation where the reswept zone is reduced in width due to bottom ray limiting.

Another program shortcoming involves an assumption that both source and receiver would be more shallow than the second DSC SVP point chosen (depth D_2). In other words, the programs were designed to allow for source/receiver depths within the mixed layer or the first isogradient layer below the SLD. After the five point SVP is entered and the gradients computed, source and receiver depths are entered and converted to velocities. The programs determine these velocities (C_S and C_R) by subtracting an appropriate amount from the velocity at the SLD. The amount subtracted is determined by depth separation from the SLD and by the gradient in either the ML or the first layer below the SLD. If source or receiver depth is greater than D_2 , sound velocity should be determined by correcting C_2 (the velocity at D_2) and by using g_2 (the second layer gradient). Since this is not done, velocities for source/receiver depths below D_2 will be in error (usually too low). Source and receiver velocity errors are carried over into Δr_S and Δr_R range corrections. If the velocities are too low, the range corrections will be too large. This is normally a rather insignificant source of total range error, however, since Δr_S and Δr_R errors will be a small fraction of the magnitude of those terms and because the range correction terms are small to begin with.

The mathematics of ray tracing in isogradient layers is quite straightforward. By Snell's Law,

$$\frac{C_1}{\cos \theta_1} = \frac{C_2}{\cos \theta_2} = \text{(A constant for each ray)} \quad (2)$$

the angle of a ray departing a layer can be determined from the angle of entry into that layer. In Eq. (2), C_1 is the sound velocity where the sound ray enters a layer, θ_1 is the angle of entry, C_2 is the sound velocity where the ray departs the layer, and θ_2 is the angle of departure.

Rays travel in circular arcs within constant gradient layers, and the radius of curvature is:

$$R = \left| \frac{C_1}{g_1 \cos \theta_1} \right| \quad (3)$$

C_1 and θ_1 are as defined above and g_1 is the gradient within the layer (in this case, layer 1).

Finally, the horizontal distance traveled by a ray while traversing a layer is:

$$\Delta r = \left| R (\sin \theta_2 - \sin \theta_1) \right| \quad (4)$$

Figure 5 demonstrates an example application of Eqs. 2 through 4. It should be noted that absolute value signs are used in Eqs. 3 and 4 because the gradient in Eq. 3 and the difference of sines in Eq. 4 may be positive or negative, while R and Δr are always positive.

The programs use these equations to compute the horizontal range increments each ray accumulates within the four layers, doubles each term (to account for the downward and

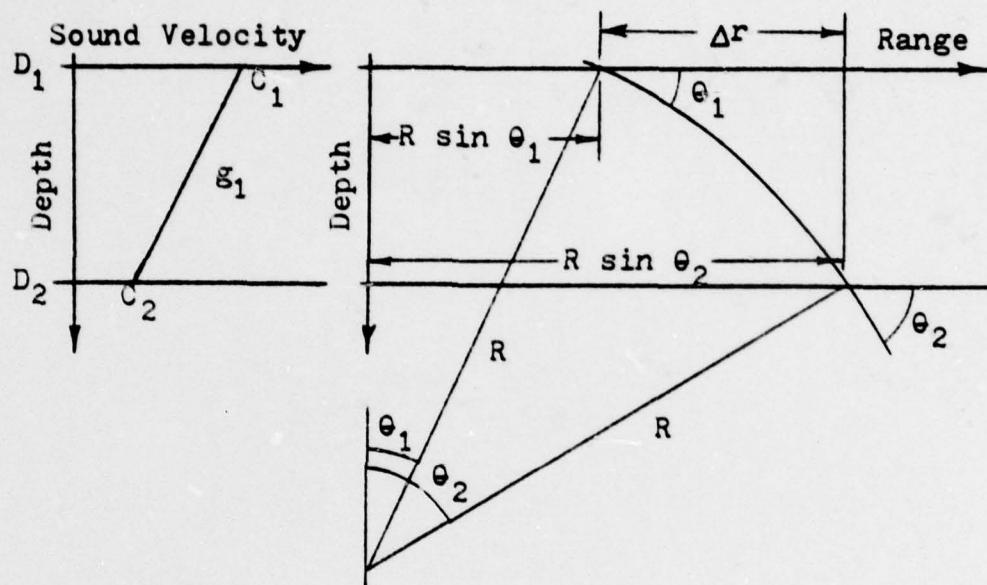


Figure 5. Horizontal Distance Traveled Within an Isogradient Layer.

upward passes through each layer), and then sums the terms to obtain cycle distances. The fourth layer requires a slightly different treatment because the rays become horizontal and then turn back upward within that layer. Essentially the same formulas are used, however. The equations are also used to compute the range correction terms.

In considering the various possible ray paths between source and receiver, it was decided there were four basic situations which could occur:

- 1) No mixed layer, both source and receiver below the SLD. (Deep/Deep)
- 2) Mixed layer present, both source and receiver below the SLD. (Deep/Deep/ML)
- 3) Mixed layer present, both source and receiver within the layer. (Shal/Shal)
- 4) Mixed layer present, source or receiver above the SLD, the other below. (Crosslayer)

The only difference between the first two cases is the mixed layer effect in case 2. That effect causes a widening of annuli due to spreading of sound rays as they travel up to the surface and back down to the SLD within the layer. The mixed layer effect is also included in the third and fourth cases above.

It was originally intended to include all four cases in one range prediction program. Again due to calculator limitations, it was necessary to use two programs to cover the four possibilities. The first range program (labeled Deep/Deep) is for cases 1) and 2) above when both source and receiver are below the SLD whether or not an ML exists. The

second range program (labeled Shal/Shal or Crosslayer) is for use in cases 3) and 4) above when source or receiver or both are above the SLD.

Formulas used to determine range to inner edge of the first CZ (RCZi) and range to the outer edge of the first CZ (RCZo) follow:

$RCZi = r_{min} - \Delta r_S - \Delta r_R$	Deep/Deep
$= r_{min} + \Delta r_S + \Delta r_R$	Shal/Shal
$= r_{min} + \Delta r_S - \Delta r_R$	Crosslayer
$RCZo = r_0 + \left\{ \begin{smallmatrix} 0 \\ 2 \Delta r_0 \end{smallmatrix} \right\} + \Delta r_S + \Delta r_R$	Deep/Deep Deep/Deep/ML
$= r_0 + 2 \Delta r_0 + \Delta r_S - \Delta r_R$	Shal/Shal
$= r_0 + 2 \Delta r_0 + \Delta r_S + \Delta r_R$	Crosslayer

In these equations, r_{min} and r_0 have been previously defined, Δr_S and Δr_R are the respective horizontal range corrections which account for source and receiver depth separation from the SLD, and $2 \Delta r_0$ is the correction for mixed layer effect. Figures 6(a) through 6(f) (not to scale) depict the RCZi and RCZo formulas in graphic form. Ranges to second and subsequent CZ annuli are taken to be integer multiples of the ranges produced.

Two items of interest, both evident in Figs. 6(a) - 6(f), are worth mentioning at this point. First, acoustical reciprocity is invoked and the more shallow of source and receiver is always treated as "source" of the sound rays within the calculator programs. Secondly, only those sound rays

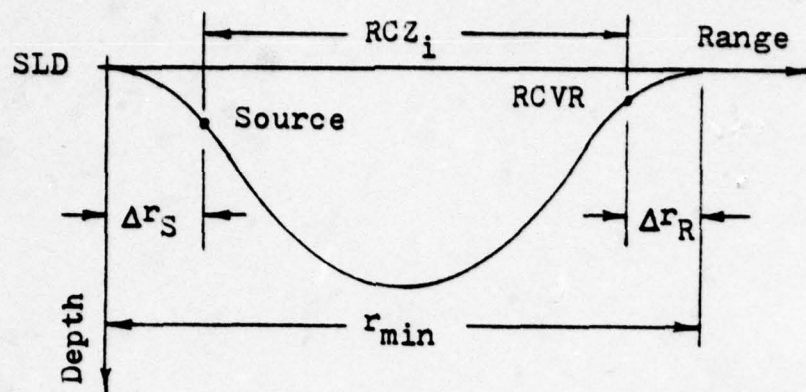


Figure 6(a). RCZ_i for Deep/Deep Case.

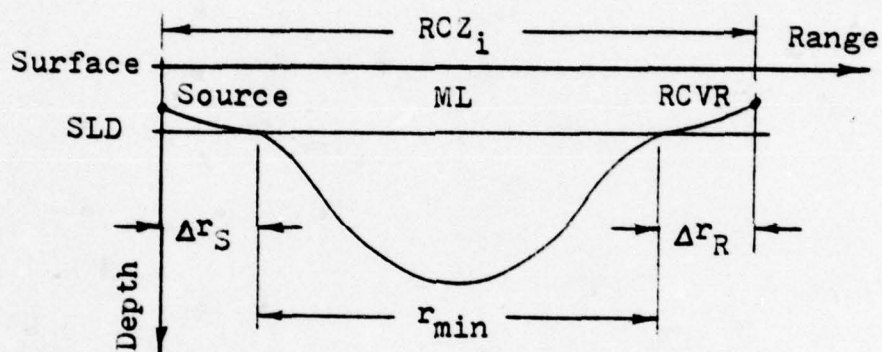


Figure 6(b). RCZ_i for Shal/Shal Case.

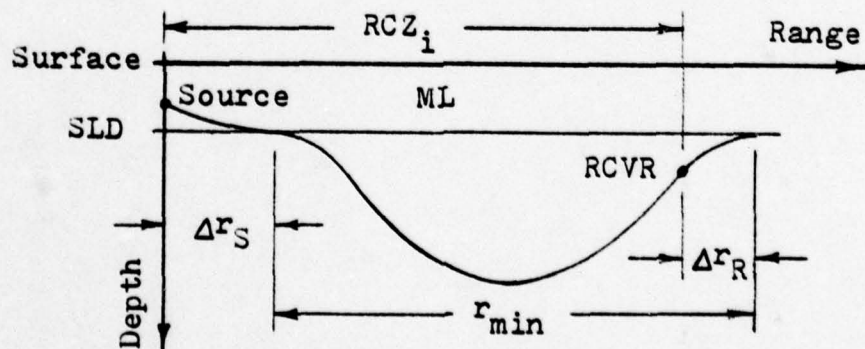


Figure 6(c). RCZ_i for Crosslayer Case.

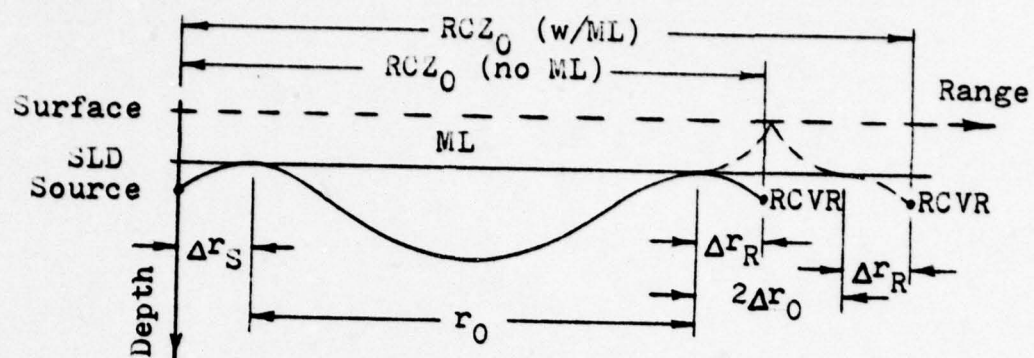


Figure 6(d). RCZ_0 for Deep/Deep Case.

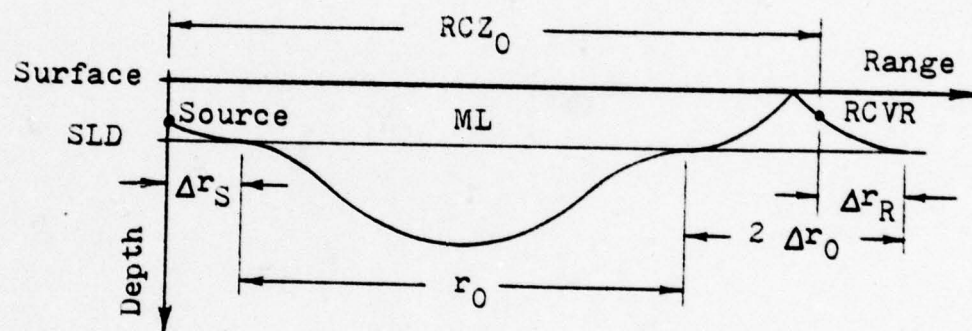


Figure 6(e). RCZ_0 for Shal/Shal Case.

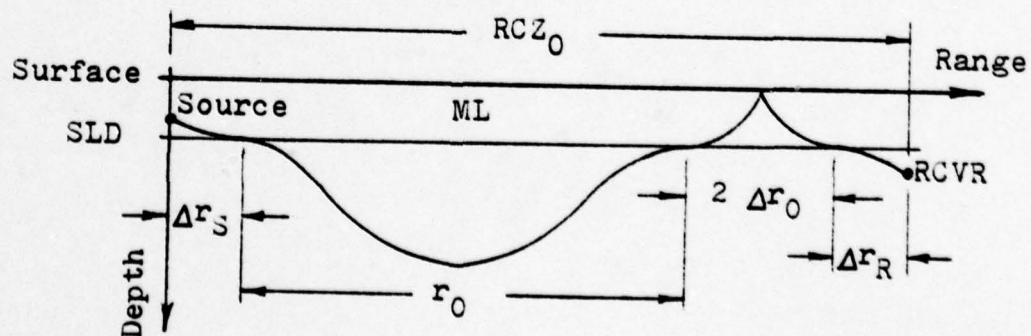


Figure 6(f). RCZ_0 for Crosslayer Case.

which experience no more than one ocean surface reflection between source and receiver are considered in this model. Both of these conventions are commonly applied to ray tracing models. Although they theoretically have little or no effect on model results, they greatly simplify the work of programming a ray tracing model.

C. CZ GAIN AND TRANSMISSION LOSS MODEL

In general, transmission loss is defined as ten times the logarithm of the ratio of sound intensities measured at one meter from a source and at range r from that source.

$$TL = 10 \log \frac{I_1}{I_r}$$

Intensity has units of power per unit area. The change in intensity between one meter and range r is due to geometric spreading of the power over a different amount of area and due to attenuation of some of the power through absorption, scattering, diffusion, etc.

In ray tracing theory, it is assumed there is no sound power transfer across sound rays. Therefore, the power flowing from a source between two sound rays remains between those rays and travels out in a direction parallel to the ray paths. Determining the portion of transmission loss due to geometric spreading (TL_g) under this assumption reduces to finding ten times the logarithm of the ratio of areas (at range r and at one meter) penetrated by the power between the two rays perpendicular to the direction of travel.

$$TL_g = 10 \log \frac{A_r}{A_1}$$

A mathematical development of this technique is contained on pages 119-121 of Ref. 1.

Figure 7 shows how this method was adapted for use in the CZ Gain and Transmission Loss portion of the calculator model developed. The area (A_1) at one meter from the source is the product of area height and area circumference. The sound rays bounding the area above and below are the minimum and maximum departure angle rays which produce the reswept zone in the CZ annulus. The angular spread of those rays ($\Delta\theta$) in radian units times the sphere radius (1 meter) is the area height. Cosine of the average angle of departure of the rays (θ_1) times the sphere radius times 2π is circumference of the area. Therefore:

$$A_1 = 2\pi \Delta\theta \cos \theta_1 (m^2)$$

In the CZ, the area (A_2) over which the same power is distributed is also found by a product of area circumference and area width. Circumference is 2π times range to the CZ (RCZi). Width of the area perpendicular to the sound rays is the product of CZ annulus width (CZW) and the sine of the average angle of arrival of the rays at the receiver depth (θ_2). Therefore:

$$A_2 = 2\pi RCZi CZW \sin \theta_2 (m^2)$$

and the geometric TL expression becomes:

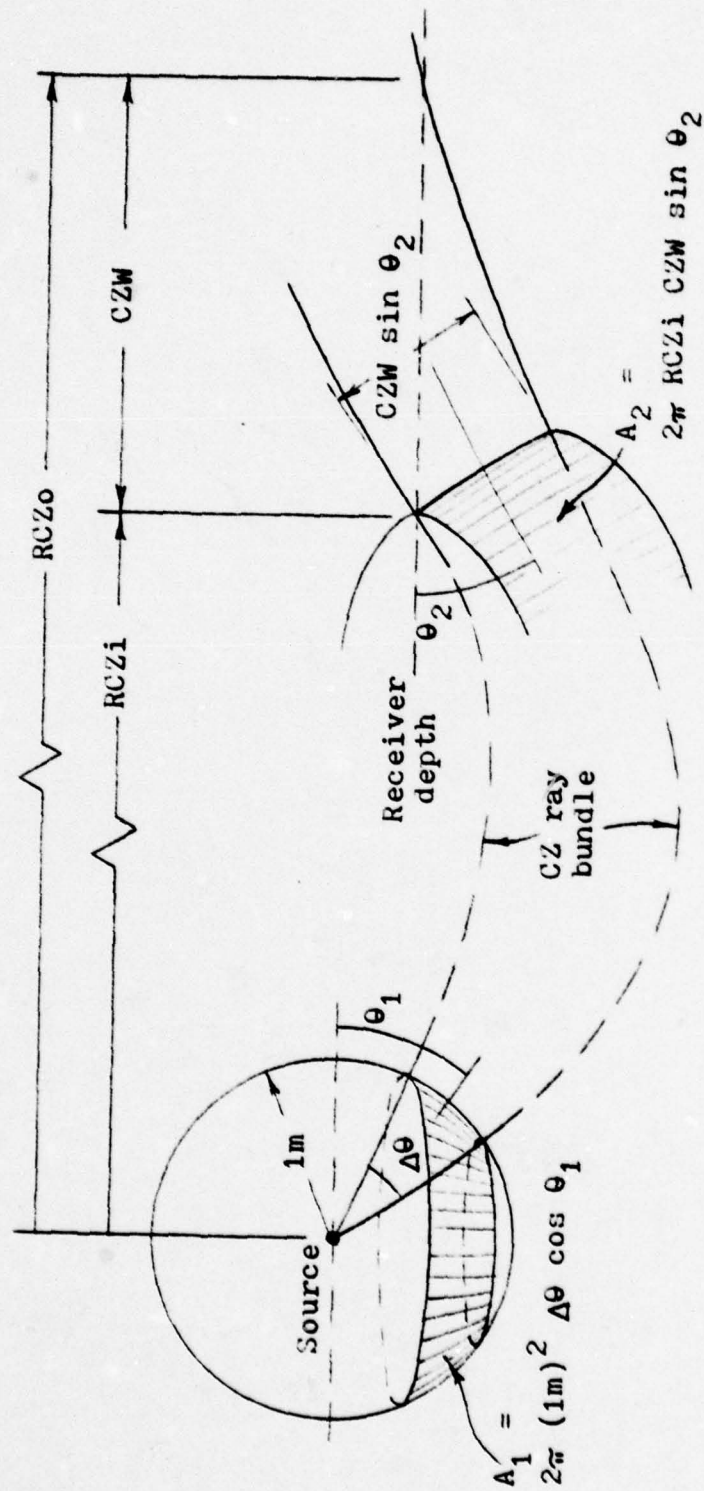


Figure 7. Geometric Transmission Loss by Ray Tracing Method.

$$TL_g = 10 \log \frac{RCZi \ CZW \ \sin \theta_2}{\Delta\theta \ \cos \theta_1}$$

Substituting this expression back into Eq. 1, which is the definition of CZ gain, and reducing to simplest form yields the algorithm used to determine G in the calculator model:

$$G = 10 \log \frac{RCZi \ \Delta\theta \ \cos \theta_1}{CZW \ \sin \theta_2} \quad (5)$$

To implement this algorithm, the program has only to determine the angular terms since RCZi and CZW are available from the range program results. After one of the range programs has been run, the user loads the G and TL program into calculator memory without altering the contents of the data storage registers left from the range program. Then the iterative ray tracing process begun in the range program is continued in the gain program. The angle of departure of sound rays from the SLD is incremented beyond θ_{rmin} (left in storage from the range program) and cycle distances produced are checked for approximate equality with r_0 . In this way, the ray which completes the reswept zone is found, and its angle of departure from the SLD is θ_{rswp} . Then θ_{rswp} and zero degrees (the angle for the ray producing cycle distance r_0) are converted to angles of departure from the source depth, θ_{SR} and θ_{SO} respectively, and angles of arrival at the receiver depth, θ_{RR} and θ_{RO} respectively, using Snell's law. The angular terms in Eq. 5 are then computed using the following formulas:

$$\begin{aligned}
\Delta\theta &= \theta_{SR} + \theta_{SO} && \text{Deep "source"} \\
&= \theta_{SR} - \theta_{SO} && \text{Shal "source"} \\
\theta_1 &= \frac{\theta_{SR} - \theta_{SO}}{2} && \text{Deep "source"} \\
&= \frac{\theta_{SR} + \theta_{SO}}{2} && \text{Shal "source"} \\
\theta_2 &= \frac{\theta_{RO} + \theta_{RR}}{2}
\end{aligned}$$

Recall that "source" in the model refers to the more shallow of source and receiver. Therefore, the deep "source" forms of these formulas are used only after using the Deep/Deep range program. In all other cases, the "source" is considered to be shallow. Figure 8 depicts these angular relationships for the various depth conditions.

It should be pointed out there are two inherent errors in the angular quantities determined. First, the possible source and receiver sound velocity errors mentioned earlier could cause the gain algorithm angles to be slightly off. This would only occur if depths greater than D_2 were entered for source or receiver or both. Secondly, θ_{rswp} is found for the ray which has cycle distance equal to r_0 at the SLD. Since the actual CZ ray bundle departs from the source depth (vice SLD) and arrives at the receiver depth (vice SLD), the ray which completes the reswept zone will probably be different than the ray used and it will have a slightly different angle crossing the SLD. These angular errors will cause the

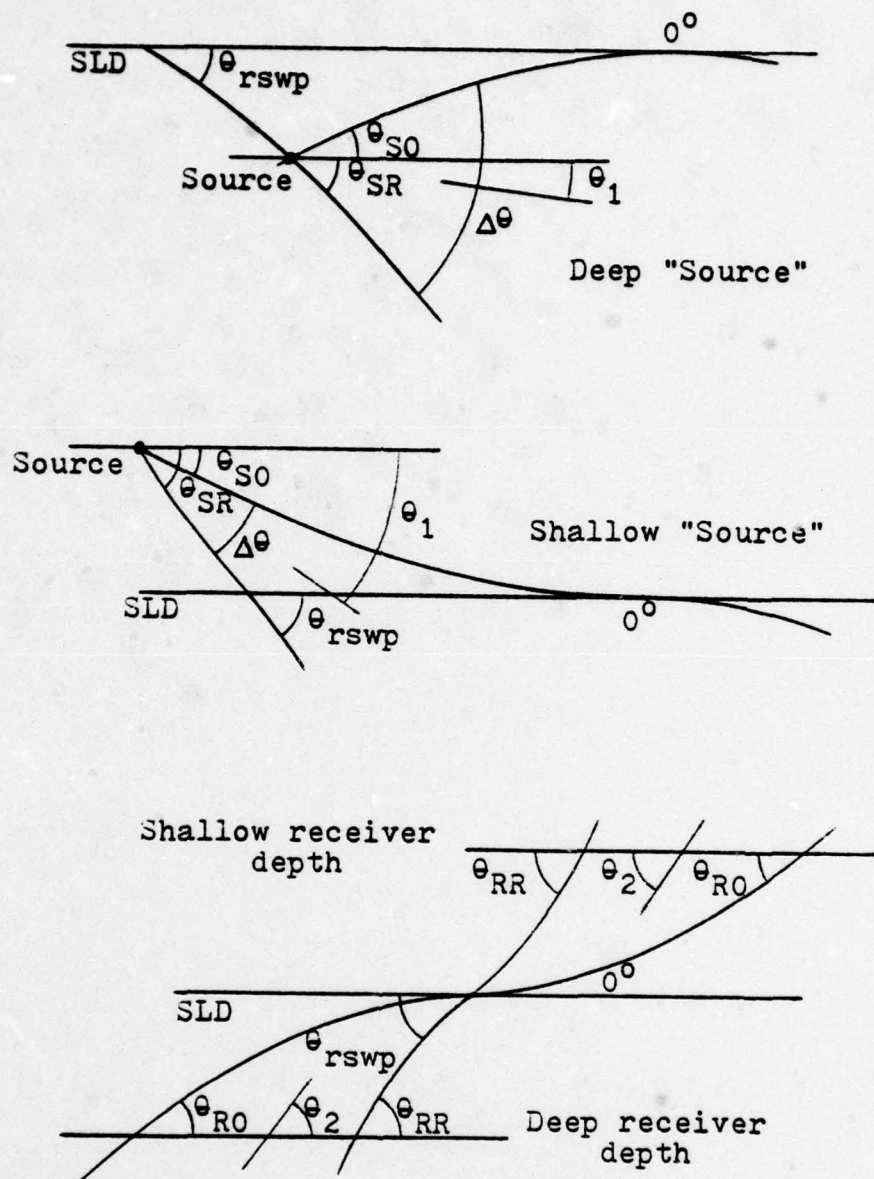


Figure 8. Determining angular terms for CZ Gain algorithm.

greatest CZ gain error in the $\sin \theta_2$ term of the algorithm. Since sine is directly proportional to angle at small angles, an error of a factor of two in θ_2 (a quite possible event) could cause a gain error of approximately 3 dB.

Once CZ gain is computed and stored, the sound frequency of interest is entered, and the attenuation coefficient is calculated using Thorpe's equation (p. 102, Ref. 1):

$$a = (0.001094) \left[\frac{0.1 f^2}{1 + f^2} + \frac{40 f^2}{4100 + f^2} \right] \quad (\text{dB/m}) \quad (6)$$

In Eq. 6, f is in kHz, and the constant in front of the expression converts attenuation coefficient from dB/kyd to dB/m. The program user enters frequency in Hz, and the program performs the conversion to kHz.

Finally, the transmission loss in the n^{th} CZ annulus for the frequency of interest (TL_n) is determined by:

$$TL_n = 20 \log (n RCZi) + z (n RCZi) - G \quad (7)$$

In this equation, the subscript n denotes the n^{th} CZ annulus, the range to which is n times $RCZi$.

After a range program is run, and after the gain portion of the G and TL_n program has been completed, TL_n values for a variety of frequencies and CZ annuli may be rapidly obtained for the SVP, source depth, and receiver depth conditions entered. If, however, a different set of source/receiver depth conditions are also of interest, the entire procedure beginning with the appropriate range program must be performed again.

D. CALCULATOR PREDICTIONS COMPARED TO ICAPS

1. Choosing the SVP Points for the Program

The five point SVP limitation of the ray tracing procedure is a rather serious handicap in many situations. Actual sound velocity profiles not only are curvilinear in overall shape but also have many small scale features and they are time varying functions. Approximating these curves with only four straight line segments presents a difficult challenge.

In general, matching the gradients, sound velocities, and associated depths are all important in choosing SVP points. The greatest potential for causing large range prediction errors occurs when the SVP contains an extensive near surface layer with very slight velocity gradient. The horizontal distance traveled by a shallow depression angle ray within such a layer varies considerably with small changes in the gradient or layer thickness. Under such conditions, then, it is extremely important to match those characteristics as closely as possible.

Another important item to carefully match is the sound velocity at the DSC axis. This velocity determines the maximum angle of depression for each ray prior to commencing upward refraction. The horizontal distance traveled by a ray below the axis is highly dependent on that angle.

Table IV contains the five point sound velocity profiles picked by the author for use in comparing the program performance to ICAPS predictions. Depths in the table

<u>5 Points</u>	<u>FEB</u>	<u>MAY</u>	<u>AUG</u>	<u>NOV</u>
		<u>PACIFIC</u>		
D1	75	10	0	30
C1	1489.8	1500.2	1508.6	1497.7
D2	340	80	100	100
C2	1480.0	1490.0	1483.0	1484.0
D3	500	600	600	600
C3	1476.2	1477.0	1475.5	1476.0
D4	1060	1600	1750	1400
C4	1480.0	1485.0	1486.5	1483.0
D5	1940	2610	3120	2460
		<u>ATLANTIC</u>		
D1	100	0	0	0
C1	1524.6	1530.9	1541.1	1535.5
D2	550	100	125	125
C2	1522.5	1522.0	1522.5	1522.5
D3	1080	575	550	625
C3	1493.0	1524.0	1524.5	1524.5
D4	1750	1225	1200	1175
C4	1495.0	1488.5	1487.5	1489.0
D ₅	3780	4175	4760	4460
		<u>MEDITERRANEAN</u>		
D1		10	0	10
C1		1526.6	1537.6	1528.7
D2		30	50	50
C2		1518.0	1517.5	1517.5
D3		100	100	125
C3		1513.0	1513.0	1512.0
D4		800	700	900
C4		1521.5	1519.5	1522.5
D5		1125	1800	1290

Table IV. Five Point Sound Velocity Profiles.
(Depths in meters, velocities in m/sec)

are in meters, and sound velocities are in meters per second. The reader may want to plot these points on the graphs of Figs. 1(a) through 1(1) so he may see how the four isogradi-ent layers picked match the ICAPS profiles. It should be pointed out that only the initial selection of SVP points was used in the subsequent comparisons of calculator model results to ICAPS predictions. Since an ASW aircrewman using the programs in attempting an in situ prediction of acoustic conditions would not be able to judge whether SVP point adjustments would improve or degrade prediction accuracy, it was felt that comparing results of the initial SVP point selection with ICAPS would be more meaningful to the objective of developing the calculator programs.

Comparing calculator model predictions to ICAPS predictions in a definitive statistical manner was not done. The main reason for this was alluded to in the preceding paragraphs. Since the SVP points entered in the calculator program must be picked subjectively by the person using the program and since it is unlikely different people would pick the exact same points off any given SVP, it is clear that calculator results can be expected to vary from operator to operator.

2. CZ Range and Annulus Width Comparisons

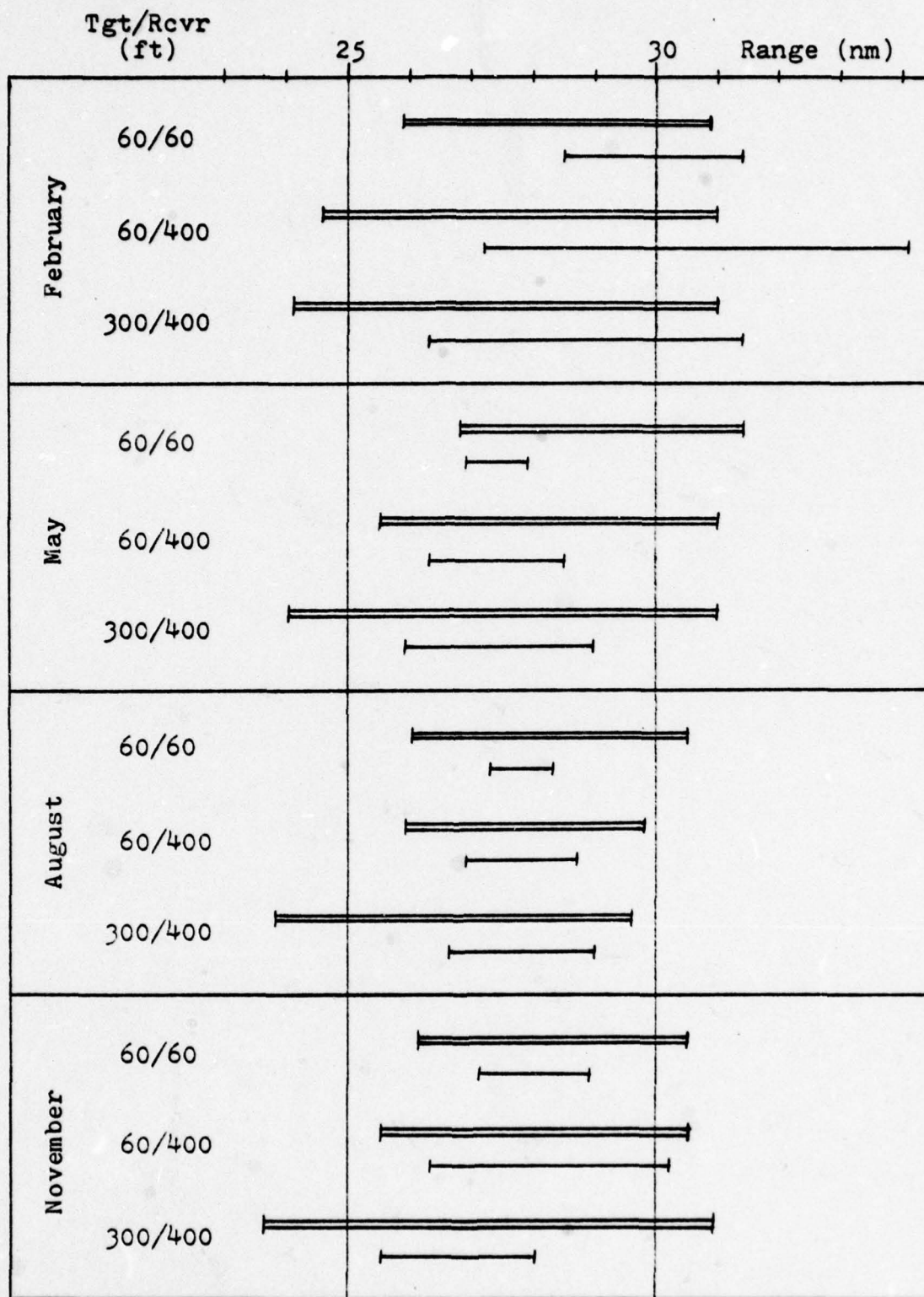
The calculator range programs produce one value each for RCZi and RCZo for any given SVP, source depth, and receiver depth situation. Under the same set of conditions, ICAPS yields four sets of RCZi and CZW values, one set for

each of the four frequencies entered. In order to compare the calculator performance to ICAPS it was first necessary to reduce the ICAPS predictions to one value each for RCZi and CZW for each SVP/source/receiver condition. This was done by simple averaging to eliminate the frequency variable from the ICAPS range and width predictions.

Figures 9(a) - 9(c) display range and width comparisons in graphical form for the Pacific, Atlantic, and Mediterranean locations respectively. In each figure the double barred lines represent the ICAPS first CZ annuli predictions (averaged over frequency), and the single barred lines represent the calculator predictions. Numerical values for inner and outer first CZ ranges may be obtained from the scales at the tops of the figures.

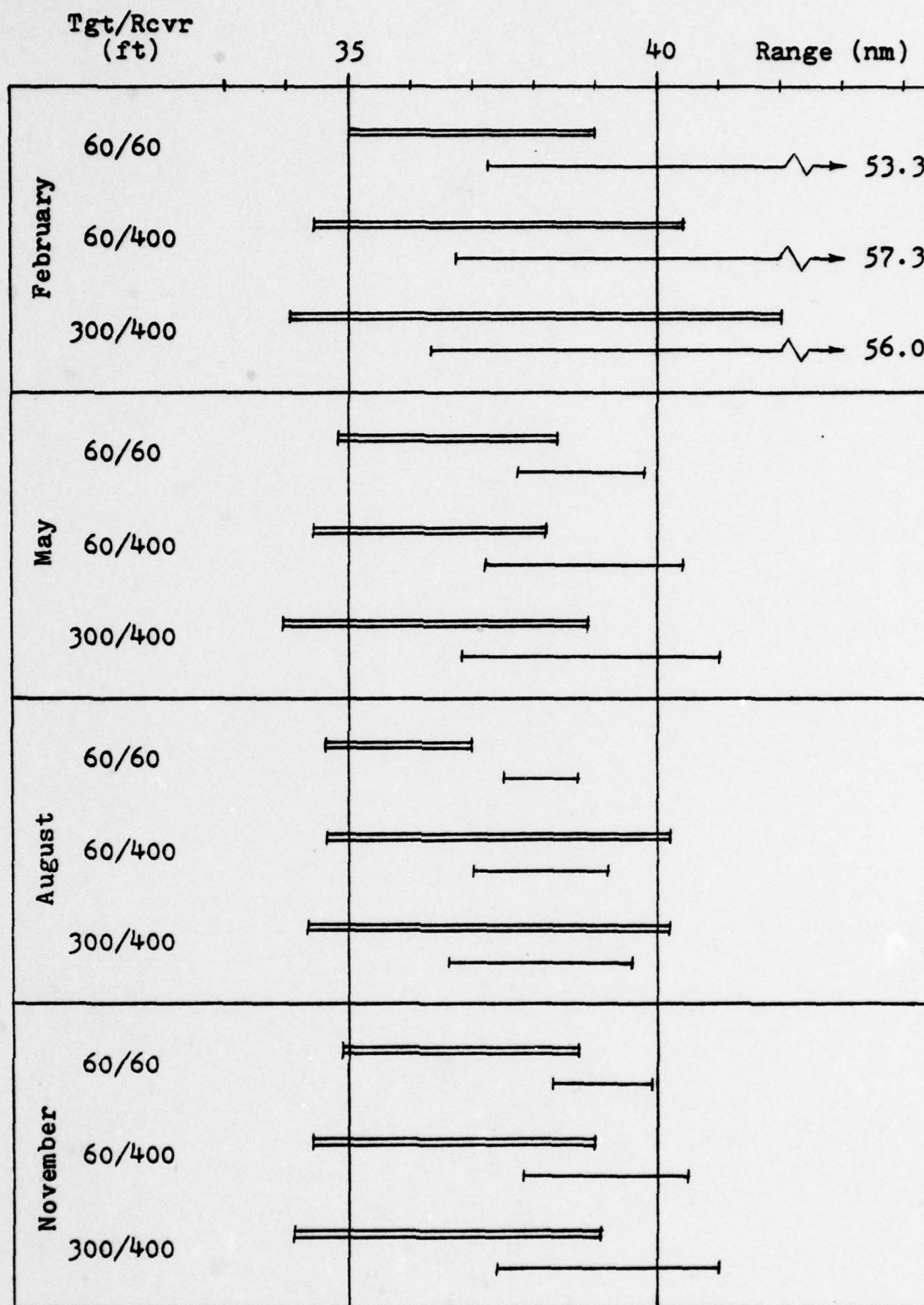
In all, there were 32 cases where these graphical comparisons could be made. The following comments pertain to those comparisons:

- a) In 30 of the 32 cases the calculator annuli overlap at least a portion of the ICAPS annuli.
- b) In 14 of the 32 cases the calculator annuli are completely contained within the limits of the ICAPS annuli.
- c) In all 32 cases RCZi ranges predicted by the calculator were greater than those predicted by ICAPS. In the 12 Pacific cases, the calculator RCZi values were approximately 1.7 nm greater than ICAPS on the average. In the 12 Atlantic cases, the average difference was approximately

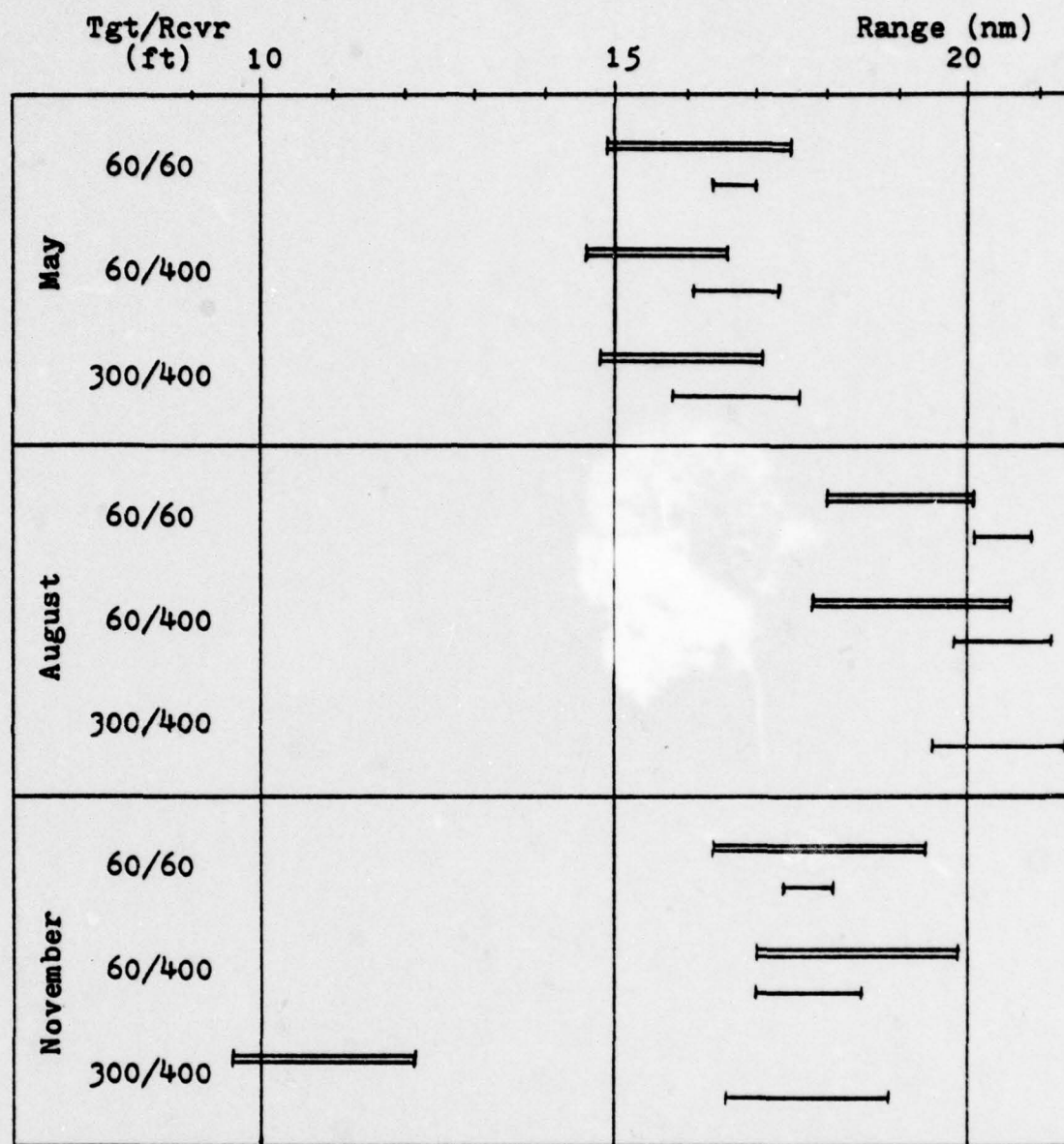


Legend: ICAPS Calculator program

Figure 9(a). Comparisons of ICAPS and Calculator CZ Annuli Predictions. Pacific Ocean.



Legend: ICAPS Calculator program
 Figure 9(b). Comparisons of ICAPS and Calculator CZ Annuli Predictions. Atlantic Ocean.



Legend: ICAPS Calculator program

Figure 9(c). Comparisons of ICAPS and Calculator C2 Annuli Predictions. Mediterranean Sea.

2.8 nm. And in the eight Mediterranean cases, 1.5 nm was the mean difference.

d) In 27 of the 32 cases the CZ width predictions from the calculator were more narrow than the ICAPS predicted widths. Three of the five cases where calculator CZW exceeded ICAPS CZW were from the February SVP in the Atlantic location. That SVP contained a very deep (500 meter), nearly isovelocity layer near the surface. In such a profile, CZ refraction produces ray paths that are spread over a very wide (in this case 16-30 nm) annulus. Only the rays which return to the SLD within the first few nm at the inner edge of that annulus experience sufficient convergence to produce detectable CZ gain, however. Going from inner to outer edge of such an annulus the CZ refracted rays rapidly fan out experiencing progressively less convergence and producing progressively less CZ gain. Additionally, if the bottom grazing ray were considered, it would be seen to limit the reswept region of this type annulus to something far less than that indicated. Since the calculator model fails to account for either of these factors, it fails rather dramatically to produce a "practical" CZ annular width from this SVP type.

In summary, the calculator model produces CZ annuli that roughly agree with those produced by ICAPS in all three ocean basins considered. Calculator RCZi ranges are 5-10% greater on the average than the ICAPS values. Calculator CZW predictions (excluding the Atlantic February SVP) are

40-50% narrower than ICAPS widths on the average. And, the Atlantic February case indicates there is at least one SVP type in which the calculator model fails to produce even marginally acceptable results for CZW.

3. CZ Gain Comparisons

As with CZ range and width comparisons, it was necessary to average the ICAPS gain data with respect to frequency before calculator gain predictions could be compared. The estimated ICAPS gain values in Tables II and III were thus reduced to one number for each SVP, source, and receiver condition. Table V, CZ Gain Prediction Comparisons, contains numbers that represent the difference between calculator gain predictions and the averaged ICAPS values. Minus signs in the table indicate those cases where calculator gain was less than the ICAPS value.

As with the range and width comparisons, the worst agreement occurred in the Atlantic winter SVP case. Since CZW is a term in the gain algorithm, the extremely wide annuli predicted by the calculator caused gain values to be far too low for the three source/receiver conditions associated with that SVP.

Excluding the Atlantic winter SVP case, the following comments can be made concerning the other 29 CZ gain comparisons:

- a) Calculator gain values ranged from 7.3 dB lower to 5 dB higher than the averaged ICAPS values.

$$\overline{G}_{ICAPS} / (G_{calc} - \overline{G}_{ICAPS})$$

SVP Profile	Source/ Receiver (ft)	Pacific	Atlantic	Mediterranean
FEB	60/60	13.4/-5.4	15.5/-10.5	
	60/400	11.4/-2.4	13.0/-7.0	
	300/400	11.2/-2.2	17.5/-11.5	
MAY	60/60	16.4/ 0.6	16.5/-0.5	14.3/ 3.7
	60/400	11.6/-2.6	14.0/-2.0	10.7/-1.7
	300/400	12.7/-0.7	15.0/-3.0	18.3/-6.3
AUG	60/60	15.8/ 2.2	16.0/ 2.0	17.7/-0.7
	60/400	12.8/-1.8	11.5/ 0.5	10.0/ 0.0
	300/400	12.4/ 0.6	14.5/-1.5	
NOV	60/60	14.0/-4.0	12.0/ 5.0	13.0/ 4.0
	60/400	11.3/-7.3	11.0/ 1.0	11.0/-3.0
	300/400	10.7/ 1.3	12.5/ 0.5	13.7/-2.7

Table V. CZ Gain Prediction Comparisons.

b) In 22 of the 29 comparisons, calculator values were within 3 dB of ICAPS.

c) In nine of the 29 comparisons calculator values were within one dB of ICAPS.

d) On the average, calculator gain values were approximately one dB less than ICAPS. This result is inconsistent with calculator CZW results in light of the gain model used. Since calculator CZW values averaged only slightly more than half the ICAPS widths, it would have been more consistent if calculator gain values turned out two to three dB higher than ICAPS (acoustic power being spread over less area in the CZ annuli, other things being equal). Perhaps an explanation for this apparent discrepancy is that the calculator model does not consider the contribution of surface reflected energy adding to the energy from upward traveling sound rays at the receiver depth. In an actual CZ annulus the downward traveling, surface reflected energy adds approximately three dB to the CZ gain over much of the annulus width. Apparently, the FACT model in the ICAPS system includes this consideration. It is also apparent that neglecting surface reflected energy in the calculator gain model has the effect of canceling errors that should result from CZW values being too narrow.

In summary of the gain results, it can be said that the ray tracing technique used in the calculator model worked reasonably well. Since three fourths of the comparison cases

resulted in gain values within three dB of the estimated ICAPS figures, TL values from the calculator displayed the same close agreement.

IV. CONCLUSIONS

A. LIMITATIONS OF THE MODEL DEVELOPED

The HP-67/97 calculators used in programming the CZ prediction model were stretched to their limits in both data storage and program step capacity. Although not known for certain, the author feels significantly more accurate results would be possible from a calculator with only moderately larger storage capacity.

The data storage limitation which allowed only five SVP points to be entered is quite restrictive and no doubt plays a large role in the CZ range and width inaccuracies obtained.

Program step capacity forced several short cuts to be taken which again would not have been necessary with a moderately larger program memory. Two separate range and width programs were required due to insufficient program space to incorporate tests for different source and receiver depth cases. Also, source and receiver depths are strictly allowed only within the upper two SVP isogradient layers because program space was not available to check for the correct layer if all depths were allowed. Additionally, and perhaps the greatest source of CZW errors observed, program step limitation prevented incorporating a method of considering the bottom limited CZ sound ray in determining the range to the outer edge of a CZ annulus. The program developed ignores the bottom entirely and considers only the reswept zone in

predicting annular width. Since calculator CZW results were considerably shorter than those indicated by ICAPS, it is assumed the discrepancy is due to not considering CZ rays beyond the reswept zone. The first priority in making improvements to the calculator model, should a larger capacity machine be implemented, would be incorporating a better method for selecting the ray which defines the outer limit of the CZ annulus.

B. USEFULNESS OF THE MODEL DEVELOPED

The degree of success in producing a useable CZ prediction model for handheld calculators must be determined by considering the objectives set forth in the first section of this study. The central idea was to ascertain if a calculator model would improve on ASRAPs CZ prediction accuracy in the case where BT conditions determined in situ differed from those used to generate the ASRAPs TL profiles. Inherent in this objective is the assumption that ASRAPs TL profiles generated primarily from climatological data would be in error due to lack of input data accuracy. Also inherently assumed is that given identical input data the calculator model would produce less accurate results than the digital computer model (FACT) used in ASRAPs (and ICAPS) due to obvious differences in data and program capacities. The real question then is a trade-off comparison: Will the basically less accurate calculator model produce better CZ predictions with actual environmental data than the more sophisticated digital computer model which had only climatological input data?

Before addressing the answer to this question, characteristics of the calculator model developed will be compared to the list of six desirable characteristics described in section I.

1. Easily available input data.

The data required are an SVP, assumed source depth, hydrophone depth, and frequency of interest. The only portion of this information not presently available to ASW aircrews is that part of the SVP below the 1,000 ft depth limit of the AN/SSQ-36 bathythermograph buoy. SVP data from the surface to 1,000 ft (the area where seasonal and diurnal variations predominantly occur) is easily obtained from the BT buoy information.

2. Ease of program operation.

Anyone familiar with HP-67/97 calculator use could operate this program without additional training.

3. Output data.

The program provides CZ annulus range and width as well as TL values for all frequencies of interest in all annuli of interest.

4. Short run time.

To run a complete program requires approximately 10 minutes once SVP data is obtained. Deploying a BT buoy and converting the temperature trace to an SVP would take an additional 10-15 minutes.

5. Based entirely on acoustic theory.

The program uses only ray tracing techniques in producing its output terms.

6. Agreement with large computer models.

Calculator CZ ranges obtained averaged 5-10% greater than ranges obtained from ICAPS. CZ width results averaged only 40-50% of those obtained from ICAPS. And, there was one SVP case studied (winter, Atlantic) in which the calculator CZW results were very different from ICAPS. That SVP case was considered a failure of the calculator model, and it must be conceded the model does not work for all CZ situations. Excluding the obvious CZW failure SVP case, TL values from the calculator averaged about one dB lower than ICAPS with extreme deviations observed ranging from -7.3dB to +5dB around the ICAPS values. Additionally, calculator results can be expected to vary from operator to operator since SVP points must be picked subjectively from an SVP graph.

Returning to the main objective of the study, the author feels that only half of the trade-off question has been answered. An easily operated, purely theoretical model was developed which works for most (but not all) CZ producing SVP conditions. And a measure of its accuracy compared to the sophisticated FACT computer model was obtained. Yet to be answered is how inaccurate ASRAPs CZ predictions are when observed BT conditions differ from climatological conditions. This portion of the question is very difficult to answer and

in fact would be a very large study in itself. Generally, inaccuracies must range over a scale from insignificant to considerable as environmental deviations range from slight to great. The most likely variables affecting degree of inaccuracy are surface water temperature, mixed layer depth, and in layer and below layer gradients. The effects of varying these or other possible factors one at a time or in various combinations on CZ range, width, and gain must be known before the entire question can be answered. Further, definite magnitudes of environmental factor deviation must be determined so that a person can judge when ASRAPS inaccuracies are likely to be greater than the calculator model inaccuracies. Until these points are answered it would be inappropriate to recommend use of the calculator model as a routine method of updating ASRAPS CZ predictions in situ.

APPENDIX

HP-67/97 Calculator Programs for Convergence Zone Range, Width and Transmission Loss Predictions

Steps required to use the programs:

1. Deploy a bathythermography buoy in the operating area of interest.
2. Convert the BT buoy information to a sound velocity profile of the upper 1,000 ft of the ocean area.
3. Combine the upper SVP data with a graph of climatological SVP data which depicts sound velocity conditions below the 1,000 ft level.
4. Pick five points from the combined SVP graph which best represent the deep sound channel portion of the SVP. The first point should be at the sonic layer depth, the fifth point at the bottom of the DSC where sound velocity equals that at the SLD, and the other three points at points on the graph such that when straight lines are drawn to connect the five points they create a linearly segmented SVP which matches the actual SVP as closely as possible.
5. Pick the appropriate CZ Range and Width program to be used as follows: If both source and receiver are below the SLD use the Deep/Deep program. If source or receiver or both are above the SLD use the Shal/Shal or Crosslayer program.
6. Load and run the appropriate Range and Width program according to the accompanying instructions.
7. Leaving the calculator power on and data storage registers unchanged, load and run the Gain and Transmission Loss program according to its instructions.

A word about units:

As currently written, the programs use metric units; meters for depths, and m/sec for sound velocities. To convert the programs for english unit input data, feet for depths and ft/sec for velocities, the conversion factor 1,852 m/nm should be changed to 6,075 ft/nm where occurring.

User Instructions for CZ Range Programs

Step	Instructions	Input	Keys	Output
1	Enter 5-point SVP which describes the Deep Sound Channel. (D_1 =SLD, D_5 =bottom of DSC.)	D_1	A	D_1
		C_1	A	C_1
		D_2	A	D_2
		C_2	A	C_2
		D_3	A	D_3
		C_3	A	C_3
		D_4	A	D_4
		C_4	A	C_4
		D_5	A	D_5
2	Press R/S to perform preliminary calculations	none	R/S	10.0
3	Enter Receiver Depth and Source Depth.	D_R	ENTER	
		D_S	R/S	RCZi
4	Range to inner edge of CZ (RCZi) and range to outer edge of CZ (RCZo) may be displayed by use of User Control keys B and C respectively. Ranges are in nautical miles.	none	B	RCZi
		none	C	RCZo

Storage Allocation for CZ Range Programs

Registers:

R0:	$D_1 / \Sigma \Delta r$	S0:	g_1	S:	$C_0 / \cos \theta_{rmin}$
R1:	C_1	S1:	g_2	B:	$\theta_{SLD} / \theta_{rmin}$
R2:	D_2 / C_S	S2:	g_3	C:	$\cos \theta_w$
R3:	C_2	S3:	g_4	D:	$\cos \theta_{w+1}$
R4:	D_3 / C_R	S4:		E:	r_w
R5:	C_3	S5:		I:	Control
R6:	$D_4 / r_{min} / RCZi$	S6:			
R7:	C_4	S7:			
R8:	$D_5 / r_0 / RCZo$	S8:			
R9:	g_0	S9:			

Initial Flag Status and Use:

- | | |
|--|---|
| 0: Off, Unused | 2: Off, set prior to r_0 calculation in Deep/Deep program only. |
| 1: Off, On if RCVR is shallow in Shal/Shal or Crosslayer program only. | 3. Off, set by data entry until r_0 is found in S/S or Crosslayer program only. |

Display Status: DSP 1

User Control Keys:

A: Data entry	a:
B: Display RCZi	b.
C: Display RCZo	c:
D:	d:
E:	e:

Step	Keys	Code	Explanation	Step	Keys	Code	Explanation
001	*LBLH	21 11	Enter data	051	R/S	51	Enter DR↑ DS
002	STO1	35 45		052	RCL0	36 00	Compute C_S
003	ISZ1	16 26 46		053	-	-45	
004	R/S	51		054	RCL1	36 45	
005	.	-62	Compute Gradients g_0	055	x	-35	
006	0	00		056	RCL1	36 01	
007	2	02		057	+	-55	
008	STO1	35 45		058	STO2	35 02	
009	ISZ1	16 26 46		059	R↓	-31	Compute C_R
010	RCL3	36 03	g_1	060	RCL0	36 00	
011	RCL1	36 01		061	-	-45	
012	RCL2	36 02		062	RCL1	36 45	
013	RCL0	36 00		063	x	-35	
014	GSB0	23 16 11	g_2	064	RCL1	36 01	
015	RCL5	36 05		065	+	-55	
016	RCL3	36 03		066	STO4	35 04	Initialize Δr routine
017	RCL4	36 04		067	SF2	16 21 02	
018	RCL2	36 02	g_3	068	1	01	
019	GSB0	23 16 11		069	STOC	35 13	$2 \Delta r_1$
020	RCL7	36 07		070	*LBL2	21 02	
021	RCL5	36 05		071	GSB0	23 16 13	
022	RCL6	36 06	g_4	072	RCL3	36 03	
023	RCL4	36 04		073	RCLC	36 13	
024	GSB0	23 16 11		074	GSB0	23 16 14	
025	RCL1	36 01	Set I=10	075	STO0	35 00	$2 \Delta r_2$
026	RCL7	36 07		076	ST+0	35-55 00	
027	RCL8	36 08		077	RCL3	36 03	
028	RCL6	36 06		078	ENT↑	-21	
029	GSB0	23 16 11		079	ENT↑	-21	$2 \Delta r_3$
030	GSB0	23 16 12	Mixed layer ?	080	RCL5	36 05	
031	RCL0	36 00		081	RCLD	36 14	
032	X=0?	16-42		082	GSB0	23 16 14	
033	GT00	22 00		083	ST+0	35-55 00	
034	STO8	35 08	If no ML, 0 to R8	084	ST+0	35-55 00	$2 \Delta r_4$
035	GT01	22 01		085	RCL5	36 05	
036	*LBL0	21 00		086	ENT↑	-21	
037	RCL9	36 09		087	ENT↑	-21	
038	x	-35	C_0	088	RCL7	36 07	
039	CHS	-22		089	RCLD	36 14	
040	RCL1	36 01		090	GSB0	23 16 14	
041	+	-55		091	ST+0	35-55 00	
042	STO0	35 11	ML present, $2 \Delta r_0$ to R8	092	ST+0	35-55 00	
043	GSB0	23 16 13		093	RCL1	36 01	
044	RCL0	36 11		094	RCLD	36 14	
045	1	01		095	+	-24	
046	GSB0	23 16 14		096	RCL1	36 45	
047	STO8	35 08	Set I=10	097	+	-24	
048	ST+8	35-55 08		098	RCLD	36 14	
049	*LBL1	21 01		099	GSB0	23 16 15	
050	GSB0	23 16 12		100	x	-35	

CZ Range Program (Deep/Deep Case)

Step	Keys	Code	Explanation	Step	Keys	Code	Explanation
101	ST+0	35-55 00		151	GSBd	23 16 14	
102	ST+0	35-55 00		152	ST+8	35-55 00	to r_0
103	GSBb	23 16 12	Set I=10	153	DSZI	16 25 46	
104	F2?	16 23 02		154	GSBc	23 16 13	
105	GT03	22 03	r_0 found ?	155	RCL4	36 04	
106	GT04	22 04		156	RCLA	36 11	to r_{min}
107	*LBL3	21 03		157	GSBd	23 16 14	
108	RCL0	36 00	Store r_0	158	ST-6	35-45 06	
109	ST+8	35-55 08	& first r_w	159	1	01	
110	1	01		160	8	08	
111	+	-55		161	5	05	Convert
112	STOE	35 15		162	2	02	RCZi & RCZo
113	*LBL4	21 04		163	ST+6	35-24 06	to nm
114	RCL0	36 00		164	ST+8	35-24 08	
115	RCL6	36 15	r_{min} found ?	165	GSBb	23 16 12	Set I=10
116	X4Y?	16-35		166	*LBLB	21 12	
117	GT05	22 05		167	RCL6	36 06	Display RCZi
118	R4	-31	Store	168	R/S	51	
119	STOE	35 15	next r_w	169	*LBLC	21 13	
120	RCLB	36 12		170	RCL8	36 08	Display RCZo
121	.	-62	Increment	171	R/S	51	
122	5	05	θ_{SLD} &	172	*LBLa	21 16 11	
123	+	-55	$\cos \theta_{SLD}$	173	-	-45	
124	ST08	35 12		174	R4	-31	Gradients
125	COS	42		175	-	-45	Subroutine
126	STOC	35 13		176	R+	16-31	
127	GT02	22 02	Next r routine	177	+	-24	
128	*LBL5	21 05	Store r_{min}	178	STOI	35 45	
129	ST06	35 06		179	ISZI	16 26 46	
130	RCLB	36 12		180	RTN	24	
131	.	-62	Initiate	181	*LBLb	21 16 12	
132	5	05	Δr_S & Δr_R	182	1	01	Set I=10
133	-	-45	corrections	183	0	00	Subroutine
134	COS	42		184	STOI	35 46	
135	STOA	35 11		185	RTN	24	
136	GSBc	23 16 13	Δr_S	186	*LBLc	21 16 13	
137	RCL2	36 02	corrections	187	RCL1	36 01	Δr
138	1	01		188	ENT1	-21	Initiation
139	GSBd	23 16 14	to r_0	189	ENT1	-21	Subroutine
140	ST+8	35-55 08		190	RTN	24	
141	DSZI	16 25 46		191	*LBLd	21 16 14	
142	GSBc	23 16 13		192	STOC	35 13	
143	RCL2	36 02		193	x	-35	Δr
144	RCLA	36 11	to r_{min}	194	X4Y	-41	Subroutine
145	GSBd	23 16 14		195	+	-24	
146	ST-6	35-45 06		196	STOD	35 14	
147	DSZI	16 25 46		197	GSBe	23 16 15	
148	GSBc	23 16 13	Δr_R	198	RCLC	36 13	
149	RCL4	36 04	corrections	199	GSBe	23 16 15	
150	1	01		200	-	-45	

CZ Range Program (Deep/Deep Case)

Step	Keys	Code	Explanation	Step	Keys	Code	Explanation
001	*LBLH	21 11	Enter data	051	RCL9	36 09	
002	STOI	35 45		052	x	-35	
003	ISZI	16 26 46		053	RCL1	36 01	
004	R/S	51		054	+	-55	
005	.	-62	Compute Gradients	055	STO2	35 02	
006	0	00		056	R↓	-31	
007	2	02		057	RCL0	36 00	
008	STOI	35 45		058	X>Y?	16-34	
009	ISZI	16 26 46	g_0	059	STO0	22 00	Set Flag 0 for shallow Receiver and Compute C_R
010	RCL3	36 03	g_1	060	STO1	22 01	
011	RCL1	36 01		061	*LBL0	21 00	
012	RCL2	36 02		062	SF1	16 21 01	
013	RCL0	36 00	g_2	063	DSZI	16 25 46	
014	GSB _a	23 16 11		064	*LBL1	21 01	
015	RCL5	36 05		065	-	-45	
016	RCL3	36 03		066	RCL1	36 45	
017	RCL4	36 04	g_3	067	x	-35	
018	RCL2	36 02		068	RCL1	36 01	
019	GSB _a	23 16 11		069	+	-55	
020	RCL7	36 07		070	STO4	35 04	
021	RCL5	36 05	g_4	071	GSB _b	23 16 12	Set I=10
022	RCL6	36 06		072	*LBL2	21 02	$2 \Delta r_1$
023	RCL4	36 04		073	GSB _c	23 16 13	
024	GSB _a	23 16 11		074	RCL3	36 03	
025	RCL1	36 01	g_4	075	RCLC	36 13	
026	RCL7	36 07		076	GSB _d	23 16 14	
027	RCL8	36 08		077	STO0	35 00	
028	RCL6	36 06		078	ST+0	35-55 00	
029	GSB _a	23 16 11	Set I=9	079	RCL3	36 03	$2 \Delta r_2$
030	9	09		080	ENT↑	-21	
031	STOI	35 46		081	ENT↑	-21	
032	RCL0	36 00		082	RCL5	36 05	$2 \Delta r_3$
033	RCL9	36 09	Compute C_0	083	RCLD	36 14	
034	x	-35		084	GSB _d	23 16 14	
035	CHS	-22		085	ST+0	35-55 00	
036	RCL1	36 01	$2 \Delta r_0$ to R8	086	ST+0	35-55 00	$2 \Delta r_4$
037	+	-55		087	RCL5	36 05	
038	STOA	35 11		088	ENT↑	-21	
039	GSB _c	23 16 13		089	ENT↑	-21	
040	RCLH	36 11	Set I=10	090	RCL7	36 07	
041	1	01		091	RCLD	36 14	
042	GSB _d	23 16 14		092	GSB _d	23 16 14	
043	STO8	35 08		093	ST+0	35-55 00	
044	ST+0	35-55 06	Enter DR DS	094	ST+0	35-55 00	
045	GSB _b	23 16 12		095	RCL1	36 01	
046	R/S	51		096	RCLD	36 14	
047	X>Y?	16-34		097	÷	-24	
048	X<Y	-41	Reciprocity test	098	RCL1	36 45	$2 \Delta r_4$
049	RCL0	36 00	Compute C_S	099	÷	-24	
050	-	-45		100	RCLD	36 14	

CZ Range Program (Shal/Shal & Crosslayer Cases)

Step	Keys	Code	Explanation	Step	Keys	Code	Explanation
101	GSBe	23 16 15		151	DSZI	16 25 46	Δr_R corrections to r_0
102	*	-35		152	GSBe	23 16 13	
103	ST+0	35-55 00		153	RCL4	36 04	
104	ST+0	35-55 00		154	1	01	
105	GSBb	23 16 12	Set I=10	155	GSBd	23 16 14	
106	F3?	16 23 03	r_0 found ?	156	DSZI	16 25 46	to r_{min}
107	GT03	22 03		157	F1?	16 23 01	
108	GT04	22 04		158	CHS	-22	
109	*LBL3	21 03	Store r_0 & first r_w	159	ST+8	35-55 00	
110	RCL0	36 00		160	GSBe	23 16 13	
111	ST+8	35-55 00		161	RCL4	36 04	
112	1	01		162	RCLA	36 11	
113	+	-55		163	GSBd	23 16 14	
114	STOE	35 15		164	F1?	16 23 01	Convert RCzi & RCzo to nm
115	*LBL4	21 04	r_{min} found ?	165	CHS	-22	
116	RCL0	36 00		166	ST-6	35-45 06	
117	RCL6	36 15		167	1	01	
118	X≠Y?	16-35		168	8	08	
119	GT05	22 05		169	5	05	
120	R4	-31	Store next r_w	170	2	02	Set I=10
121	STOE	35 15		171	ST+6	35-24 06	
122	RCL6	36 12	Increment θ_{SLD} & $\cos \theta_{SLD}$	172	ST+8	35-24 08	
123	.	-62		173	GSBb	23 16 12	
124	5	05		174	*LBLB	21 12	Display RCzi
125	+	-55		175	RCL6	36 06	
126	STOB	35 12		176	R/S	51	Display RCzo
127	COS	42		177	*LBLC	21 13	
128	STOC	35 13		178	RCL8	36 08	
129	GT02	22 02	Next r routine	179	R/S	51	Gradients Subroutine
130	*LBL5	21 05	Store r_{min}	180	*LBLa	21 16 11	
131	ST06	35 06		181	-	-45	
132	RCLB	36 12	Initiate Δr_S & Δr_R corrections	182	R4	-31	
133	.	-62		183	-	-45	
134	5	05		184	R↑	16-31	
135	-	-45		185	+	-24	Set I=10 Subroutine
136	COS	42		186	ST0i	35 45	
137	STOA	35 11		187	ISZI	16 26 46	
138	GSBe	23 16 13	Δr_S corrections to r_0	188	RTN	24	
139	RCL2	36 02		189	*LBLb	21 16 12	Δr Initiation Subroutine
140	1	01		190	1	01	
141	DSZI	16 25 46		191	0	00	
142	GSBd	23 16 14		192	STOI	35 46	
143	DSZI	16 25 46		193	RTN	24	
144	ST+8	35-55 00		194	*LBLc	21 16 13	
145	GSBe	23 16 13	to r_{min}	195	RCL1	36 01	
146	RCL2	36 02		196	ENT↑	-21	
147	RCLA	36 11		197	ENT↑	-21	
148	GSBd	23 16 14		198	RTN	24	
149	ST+6	35-55 06		199	*LBLd	21 16 14	
150	F1?	16 23 01		200	STOC	35 13	

CZ Range Program (Shal/Shal & Crosslayer Cases)

CZ Range Program (Shal/Shal & Crosslayer Cases)

User Instructions for CZ Gain and Transmission Loss Program

Step	Instructions	Input	Keys	Output
1	Run one of the CZ Range Programs. Leave the calculator on and all of the data storage registers unchanged.			
2	Load the CZ Gain and Transmission Loss Program.			
3	Enter a zero if the Shal/Shal or Crosslayer program was used, or enter a one if the Deep/Deep program was used.	0 or 1	A	G (dB)
4	Enter a frequency of interest in Hz.	f (Hz)	B	a (dB/m)
5	Enter the number of a CZ annulus of interest. (Step 5 may be repeated for as many CZ annuli as desired.)	n	C	TL _n (dB)
6	To determine the TL _n values for different frequencies, return to step 4.			

Storage Allocation for CZ Gain and Transmission Loss Program

Registers:

R0: Δr	S0: g_1	A: $\theta_{SO} / \theta_{RO} / f^2$
R1: C_1	S1: g_2	B: $\theta_{SLD} / \theta_{rswp}$
R2: C_S	S2: g_3	C: $\cos \theta_w /$
R3: C_2	S3: g_4	$\cos \theta_{rswp}$
R4: C_R	S4: a terms	D: $\cos \theta_{w+1}$
R5: C_3	S5:	E: $r_0 / \theta_{SR} / \theta_{RR}$
R6: RCZi	S6:	I: Control
R7: C_4 / a	S7:	
R8: RCZo	S8:	
R9: G terms / G	S9:	

Initial Flag Status and Use:

0: Off, On for shallow sound source.	2: Off, unused.
1: Off, On to decrease the increments used in finding θ_{SLD} .	3: Off, set by data entry until r_0 found.

Display Status: DSP 0

User Control Keys:

A: Compute G	a:
B: Compute a	b:
C: Compute TL_n	c:
D:	d:
E:	e:

Step	Keys	Code	Explanation	Step	Keys	Code	Explanation
001	*LELM	21 11	Set F0 for Shal Source	051	1	01	Large θ_{SLD} increment
002	X=0?	16-43		052	+	-55	
003	SF0	16 21 00		053	GT03	22 03	
004	1	01	Initialize r routine	054	*LBL1	21 01	First small increment of θ_{SLD}
005	STOC	35 13		055	SF1	16 21 01	
006	*LBL0	21 00		056	RCLB	36 12	
007	RCL1	36 01	$2 \Delta r_1$	057	.	-62	
008	ENT↑	-21		058	9	09	
009	ENT↑	-21		059	-	-45	
010	RCL3	36 03		060	GT03	22 03	θ_{rswp} found ?
011	RCLC	36 13		061	*LBL2	21 02	
012	GSB _a	23 16 11		062	X>Y?	16-34	
013	ST00	35 00	$2 \Delta r_2$	063	GT04	22 04	Small θ_{SLD} increment
014	RCL3	36 03		064	RCLB	36 12	
015	ENT↑	-21		065	.	-62	
016	ENT↑	-21		066	1	01	Store new θ_{SLD} & $\cos \theta_{SLD}$
017	RCL5	36 05		067	+	-55	
018	RCLD	36 14	$2 \Delta r_3$	068	*LBL3	21 03	
019	GSB _a	23 16 11		069	ST0B	35 12	
020	ST+0	35-55 00		070	COS	42	
021	RCL5	36 05		071	STOC	35 13	
022	ENT↑	-21	$2 \Delta r_4$	072	GT00	22 00	Convert RCZi & RCZo to meters
023	ENT↑	-21		073	*LBL4	21 04	
024	RCL7	36 07		074	1	01	
025	RCLD	36 14		075	8	08	
026	GSB _a	23 16 11		076	5	05	
027	ST+0	35-55 00	$2 \Delta r_4$	077	2	02	
028	RCL1	36 01		078	STx6	35-35 06	Store $\cos \theta_{rswp}$
029	RCLD	36 14		079	STx8	35-35 08	
030	÷	-24		080	RCLB	36 12	
031	RCLi	36 45		081	COS	42	
032	÷	-24	$2 \Delta r_4$	082	STOC	35 13	θ_{SR}
033	RCLD	36 14		083	PCL2	36 02	
034	GSB _b	23 16 12		084	x	-35	
035	x	-35		085	RCL1	36 01	
036	ST+0	35-55 00		086	÷	-24	θ_{SO} (negative if source shal)
037	ST+0	35-55 00	Set I=10	087	COS ⁻¹	16 42	
038	1	01		088	STOE	35 15	
039	0	00		089	RCL2	36 02	
040	ST01	35 46	Store r_0	090	RCL1	36 01	
041	RCL0	36 00		091	÷	-24	$\Delta \theta$
042	F3?	16 23 03		092	COS ⁻¹	16 42	
043	STOE	35 15	Check for Small inc. of θ_{SLD}	093	F0?	16 23 00	
044	RCLC	36 15		094	CHS	-22	
045	XZY	-41		095	ST0A	35 11	
046	F1?	16 23 01		096	+	-55	
047	GT02	22 02	Decrease θ_{SLD} inc. ?	097	D+R	16 45	
048	XZY?	16-34		098	ST0S	35 09	
049	GT01	22 01		099	RCLC	36 15	
050	RCLB	36 12		100	RCLA	36 11	

CZ Gain and Transmission Loss Program

Step	Keys	Code	Explanation	Step	Keys	Code	Explanation
101	-	-45	$\cos \theta_1$	151	4	04	Second term
102	2	02		152	1	01	
103	\div	-24		153	0	00	
104	COS	42		154	0	00	
105	ST \times 9	35-35 09		155	RCLA	36 11	
106	RCLC	36 13	θ_{RR}	156	+	-55	Store a
107	RCL4	36 04		157	\div	-24	
108	\times	-35		158	Σ +	56	
109	RCL1	36 01		159	RCLZ	36 56	
110	\div	-24		160	ST07	35 07	
111	COS $^{-1}$	16 42	θ_{RO}	161	Σ -	16 56	(Clear S4)
112	RCL4	36 04		162	1	01	Convert a from dB/kyd to dB/m
113	RCL1	36 01		163	.	-62	
114	\div	-24		164	0	00	
115	COS $^{-1}$	16 42		165	9	09	
116	+	-55	θ_2	166	4	04	
117	2	02		167	EEX	-23	Display a
118	\div	-24		168	3	03	
119	SIN	41	$\sin \theta_2$	169	CHS	-22	
120	ST \div 9	35-24 09		170	ST \times 7	35-35 07	
121	RCL8	36 08		171	RCL7	36 07	
122	RCL6	36 06	RCZi	172	R/S	51	nRCZi
123	ST \times 9	35-35 09	CZW	173	*LBLC	21 13	
124	-	-45		174	RCL6	36 06	
125	ST \div 9	35-24 09		175	\times	-35	
126	RCL9	36 09	Compute and Display G	176	ENT \uparrow	-21	
127	LOG	16 32		177	LOG	16 32	20log(nRCZi)
128	1	01		178	2	02	
129	0	00		179	0	00	
130	\times	-35		180	\times	-35	a(nRCZi)
131	ST09	35 09		181	\times Y	-41	
132	R/S	51		182	RCL7	36 07	
133	*LBLB	21 12	Convert f to kHz	183	\times	-35	Compute & Display TL_n
134	EEX	-23		184	+	-55	
135	3	03		185	RCL9	36 09	
136	\div	-24	Store f^2	186	-	-45	
137	\times^2	53		187	R/S	51	
138	ST0A	35 11	Attenuation Coefficient	188	*LBLa	21 16 11	Δr Subroutine
139	.	-62		189	ST0C	35 13	
140	1	01		190	\times	-35	
141	\times	-35		191	\times Y	-41	
142	1	01		192	\div	-24	
143	RCLA	36 11	First term	193	ST0D	35 14	
144	+	-55		194	GSBb	23 16 12	
145	\div	-24		195	RCLC	36 13	
146	Σ +	56		196	GSBb	23 16 12	
147	4	04		197	-	-45	
148	0	00		198	\times	-35	
149	RCLA	36 11		199	RCLC	36 13	
150	\times	-35		200	\div	-24	

CZ Gain and Transmission Loss Program

AD-A072 050

NAVAL POSTGRADUATE SCHOOL MONTEREY CA
CONVERGENCE ZONE PREDICTION MODELS WITH PROGRAMS FOR USE ON HP---ETC(U)
MAR 79 R L BADGER

F/G 9/2

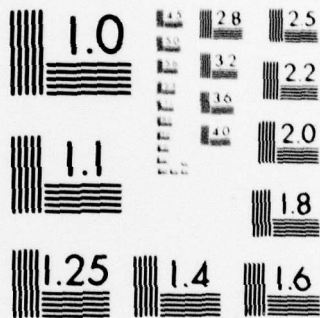
UNCLASSIFIED

NL

2 OF 2
AD
A072050



END
DATE
FILMED
9-79
DDC



MICROCOPY RESOLUTION TEST CHART
NATIONAL BUREAU OF STANDARDS-1963-A

LIST OF REFERENCES

1. Urlick, R. J., Principles of Underwater Sound, p. 114-121, McGraw-Hill, 1975.
2. Beckes, M. E., Burhans, N. P., and Gump, R. E., Passive Environmental ASW Prediction System (PEAPS), Master's Thesis, Naval Postgraduate School, Monterey, California, March 1975.
3. Madden, L. D., POCKET-PROPLOSS Programs and Models for the Computation of Acoustic Transmission Loss on Hand-Held Calculators, Master's Thesis, Naval Postgraduate School, Monterey, California, March 1977.
4. U. S. Naval Oceanographic Office Report TN 3700-57-77, User's Manual for the Integrated Carrier ASW Prediction System (ICAPS), by J. D. Pennylegion, p. 9, 10, B-1 - B-4, C-1 - C-3, January 1977.
5. Maury Center for Ocean Science Report 109, The FACT Model, Volume I, by C. W. Spofford, p. 2-7, 2-8, 3-7, November 1974.

INITIAL DISTRIBUTION LIST

	No. Copies
1. Defense Documentation Center Cameron Station Alexandria, Virginia 22314	2
2. Navy Tactical Support Activity P. O. Box 1042 Silver Springs, Maryland 20910	2
3. Library, Code 0142 Naval Postgraduate School Monterey, California 93940	2
4. Associate Professor A. B. Coppens Code 61Cz Department of Physics and Chemistry Naval Postgraduate School Monterey, California 93940	1
5. Associate Professor R. H. Shudde Code 55Su Department of Operations Research Naval Postgraduate School Monterey, California 93940	5
6. COMPATWINGSPAC Attn: Code 51 Naval Air Station Moffett Field, California 94035	1
7. COMPATWINGSLANT Attn: Code N7 Naval Air Station Brunswick, Maine 04011	1
8. Commander Antisubmarine Warfare Wing Pacific Naval Air Station North Island San Diego, California 92135	1
9. COMSEABASEDASWWINGSLANT Attn: TD&E Officer Naval Air Station Jacksonville, Florida 32228	1
10. Commanding Officer (ATTN: LCDR R.L. Badger) Patrol Squadron FIFTY FPO San Francisco 96601	1

No. Copies

11. Project Manager	1
Antisubmarine Warfare Systems Project (PM-4)	
Department of the Navy	
Washington, D.C. 20360	